

1 **Towards understanding the variability in biospheric**  
2 **CO<sub>2</sub> fluxes: using FTIR spectrometry and a chemical**  
3 **transport model to investigate the sources and sinks of**  
4 **carbonyl sulfide and its link to CO<sub>2</sub>**

5  
6 **Y. Wang<sup>1</sup>, N. M. Deutscher<sup>1,2</sup>, M. Palm<sup>1</sup>, T. Warneke<sup>1</sup>, J. Notholt<sup>1</sup>, I. Baker<sup>3</sup>, J. Berry<sup>4</sup>,**  
7 **P. Suntharalingam<sup>5</sup>, N. Jones<sup>2</sup>, E. Mahieu<sup>6</sup>, B. Lejeune<sup>6</sup>, J. Hannigan<sup>7</sup>, S. Conway<sup>8</sup>,**  
8 **J. Mendonca<sup>8</sup>, K. Strong<sup>8</sup>, J. E. Campbell<sup>9</sup>, A. Wolf<sup>10</sup>, and S. Kremser<sup>11</sup>**

9 [1] Institute of Environmental Physics, University of Bremen, Bremen, Germany

10 [2] Centre for Atmospheric Chemistry, School of Chemistry, University of Wollongong,  
11 Wollongong, Australia

12 [3] Colorado State University, Fort Collins, CO, USA

13 [4] Carnegie Institute of Washington, Stanford, CA, USA

14 [5] University of East Anglia, Norwich, UK

15 [6] Institute of Astrophysics and Geophysics, University of Liège, Liège, Belgium

16 [7] National Center for Atmospheric Research, Boulder, CO, USA

17 [8] Department of Physics, University of Toronto, Toronto, Canada

18 [9] University of California, Merced, CA, USA

19 [10] Princeton University, Princeton, NJ, USA

20 [11] Bodeker Scientific, Alexandra, New Zealand

21 Correspondence to: Y. Wang (w\_yuting@iup.physik.uni-bremen.de)

22

23 **Abstract**

24 Understanding carbon dioxide (CO<sub>2</sub>) biospheric processes is of great importance because the  
25 terrestrial exchange drives the seasonal and inter-annual variability of CO<sub>2</sub> in the atmosphere.

1 Atmospheric inversions based on CO<sub>2</sub> concentration measurements alone can only determine net  
2 biosphere fluxes, but not differentiate between photosynthesis (uptake) and respiration  
3 (production). Carbonyl sulfide (OCS) could provide an important additional constraint: it is also  
4 taken up by plants during photosynthesis but not emitted during respiration, and therefore is a  
5 potential means to differentiate between these processes. Solar absorption Fourier Transform  
6 InfraRed (FTIR) spectrometry allows for the retrievals of the atmospheric concentrations of both  
7 CO<sub>2</sub> and OCS from measured solar absorption spectra. Here, we investigate co-located and quasi-  
8 simultaneous FTIR measurements of OCS and CO<sub>2</sub> performed at five selected sites located in the  
9 Northern Hemisphere. These measurements are compared to simulations of OCS and CO<sub>2</sub> using a  
10 chemical transport model (GEOS-Chem). The coupled biospheric fluxes of OCS and CO<sub>2</sub> from  
11 the simple biosphere model (SiB) are used in the study. The CO<sub>2</sub> simulation with SiB fluxes  
12 agrees with the measurements well, while the OCS simulation reproduced a weaker drawdown  
13 than FTIR measurements at selected sites, and a smaller latitudinal gradient in the Northern  
14 Hemisphere during growing season when comparing with HIPPO (HIAPER Pole-to-Pole  
15 Observations) data spanning both hemispheres. An offset in the timing of the seasonal cycle  
16 minimum between SiB simulation and measurements is also seen. Using OCS as a  
17 photosynthesis proxy can help to understand how the biospheric processes are reproduced in  
18 models and to further understand the carbon cycle in the real world.

19

## 20 **1. Introduction**

21 Understanding the carbon dioxide (CO<sub>2</sub>) biospheric processes within the carbon cycle is of great  
22 importance, because: (1) the land carbon sink absorbs more than a quarter of the CO<sub>2</sub> emissions  
23 released by human activities, which mitigates the increase of atmospheric CO<sub>2</sub> concentration; and  
24 (2) terrestrial exchange drives CO<sub>2</sub> variability in the atmosphere on seasonal and inter-annual  
25 time scales. The total biospheric CO<sub>2</sub> flux (net ecosystem production, NEP) is the sum of two  
26 much larger terms with different seasonality and drivers: the carbon uptake of gross primary  
27 production (GPP) and the release via respiration (Re). These fluxes are co-located, therefore,  
28 typically only information about their sum (the NEP) is available when they are quantified. To  
29 improve our knowledge of CO<sub>2</sub> biospheric processes, in particular how ecosystems will respond  
30 to a changing climate, we would ideally like to understand the individual contributions of these  
31 two fluxes.

1 Laboratory experiments (e.g. Goldan et al., 1988) have studied the pathway for carbonyl sulfide  
2 (OCS) uptake by plants, which is similar to the uptake mechanism of CO<sub>2</sub> during photosynthesis.  
3 Unlike CO<sub>2</sub>, OCS uptake is a one-way process, and it is not emitted during respiration. Therefore  
4 OCS could be used to differentiate between photosynthesis and respiration fluxes of CO<sub>2</sub>  
5 (Campbell et al., 2008). Flask measurements of OCS in the Northern Hemisphere show a clear  
6 seasonal variation with a maximum in early spring and minimum in autumn, which is similar to  
7 the seasonality of CO<sub>2</sub> (Montzka et al., 2007) as biospheric fluxes are the main driver of the  
8 seasonal cycles for both species (Kettle et al., 2002a).

9 However, our knowledge about the sources and sinks of OCS remains limited. The estimates for  
10 the global budget still have significant uncertainties. This makes it difficult to use OCS as a  
11 photosynthetic tracer. The identified OCS sources include ocean emissions (direct emission and  
12 indirect emission via oxidation of carbon disulfide (CS<sub>2</sub>) and dimethyl sulfide (DMS)),  
13 anthropogenic releases (direct emission and indirect emission via oxidation of CS<sub>2</sub>), biomass  
14 burning, and volcanoes. The sinks are plant uptake, soil uptake, reaction with hydroxyl radicals  
15 (OH), reaction with oxygen atoms (O), and photolysis in the stratosphere. The ocean is believed  
16 to be the most important source of OCS via both direct and indirect fluxes, and makes the biggest  
17 contribution to the seasonality of OCS in the Southern Hemisphere (Kettle et al., 2002a). Plant  
18 uptake is commonly recognized as the main sink of OCS, and is the dominant driver of seasonal  
19 variation in the Northern Hemisphere (Goldan et al., 1988). Kettle et al. (2002a) analyzed OCS  
20 monthly fluxes, and then calculated the global annual sources and sinks, which are in balance  
21 within uncertainties. More recent studies (Suntharalingam et al., 2008; Berry et al., 2013)  
22 indicated that the plant uptake in Kettle's estimation is too small, and therefore a corresponding  
23 increase in sources is necessary to maintain the annual balance in the OCS budget. New studies  
24 have also shown that the ocean and anthropogenic sources of OCS have been underestimated  
25 (Guo et al., 2010; Berry et al., 2013; Campbell et al., 2015; Cheng et al., 2015; Launois et al.,  
26 2015a) in Kettle et al. (2002a). The disagreement between measurements and simulations of OCS  
27 indicated that the missing sources are mainly in the tropical region (Berry et al. 2013).  
28 Anthropogenic emissions are unlikely to be the main reason for missing sources in that region,  
29 and therefore ocean sources are likely to be responsible. Indeed, the ocean fluxes have large  
30 uncertainties. The direct ocean flux has large temporal and spatial variations, and under certain  
31 conditions could also act as a sink for OCS (Xu et al., 2001). Seawater measurements in some  
32 regions of the ocean suggested that the open ocean could be a small source of OCS (Weiss et al.,

1 1995; Xu et al., 2001), and that indirect ocean emissions may play more important roles. Launois  
2 et al. (2015a) calculated the direct ocean emissions using an ocean general circulation and  
3 biogeochemistry model, and estimated a source of about 813 Gg S year<sup>-1</sup>. In addition, OCS soil  
4 uptake still has large uncertainties. Some soil types act as a source (Whelan et al., 2013) or only a  
5 small sink (Xu et al., 2002; Steinbacher et al., 2004); however, the overall role of soils is as a sink  
6 of OCS, with very different uptake rates between soil types and other physical parameters (Van  
7 Diest and Kesselmeier, 2008; Sun et al., 2015). Another method to calculate the soil uptake is to  
8 use the similarity of deposition to soils between molecular hydrogen (H<sub>2</sub>) and OCS (Belviso et al.,  
9 2013; H. Chen, private communication). This estimation yields a sink of about 500 Gg S year<sup>-1</sup>,  
10 largely dependent on the H<sub>2</sub> spatial distribution (Launois et al., 2015b). Therefore, improving the  
11 estimation of the OCS sources and sinks is important when using it to investigate the biospheric  
12 fluxes of CO<sub>2</sub>. To achieve this aim, more OCS measurements at different latitudes and ecosystem  
13 regions are needed to validate the estimates.

14 Until now, the measurements used for OCS studies are sparse. The typical measurements  
15 involved, such as the NOAA/ESRL/GMD network, include ground-based and aircraft flask  
16 sampling data. These ground-based in-situ measurements are only at limited sites and aircraft  
17 measurements cover relatively short time periods. The emerging of the remote sensing data,  
18 including ground-based (Notholt et al., 2003) and satellite (Barkley et al., 2008; Kuai et al., 2014;  
19 Kuai et al., 2015; Glatthor et al., 2015) measurements, will potentially increase the number of  
20 OCS measurements largely. The satellite data provide a wide distribution of OCS; however, they  
21 are mainly sensitive in the upper troposphere and stratosphere (Barkley et al., 2008; Glatthor et  
22 al., 2015) or mid troposphere (Kuai et al., 2014), and therefore have little help on constraining the  
23 land fluxes. Ground-based solar absorption Fourier Transform InfraRed (FTIR) spectrometry  
24 measures the absorption of both CO<sub>2</sub> and OCS. This can be used to retrieve the total and/or  
25 partial atmospheric columns of these two gases. Compared to satellite retrievals, ground-based  
26 FTIR OCS retrievals are also sensitive to low altitude and can therefore more directly capture the  
27 variations due to the biospheric processes.

28 There are two networks of ground-based Fourier Transform InfraRed Spectrometers, both  
29 recording high resolution solar absorption spectra: the Total Carbon Column Observing Network  
30 (TCCON) (<http://www.tccon.caltech.edu>; Wunch et al., 2011), concentrating on CO<sub>2</sub> and  
31 methane in the near-infrared (NIR); and the Network for the Detection of Atmospheric

1 Composition Change InfraRed Working Group (NDACC-IRWG), measuring spectra in the mid-  
2 infrared (MIR). CO<sub>2</sub> total columns are retrieved from NIR spectra, while OCS profiles and  
3 columns can be calculated from MIR spectra using dedicated software packages. CO<sub>2</sub> could also  
4 be retrieved from MIR spectra, but the retrieval sensitivity dominates in the stratosphere, and  
5 therefore the CO<sub>2</sub> seasonal cycle cannot be well captured (Barthlott et al., 2015; Buschmann et al.,  
6 2015). We will only use TCCON CO<sub>2</sub> product in this study. The NDACC-IRWG sites provide a  
7 potential database of OCS, that could be used to assess its sources and sinks. Kettle et al. (2002b)  
8 used FTIR OCS total column measurements to estimate hemisphere-integrated OCS flux and  
9 confirmed their understanding of OCS global budget. However, the measurements could not put  
10 constraints on the relative magnitude of vegetative uptake and ocean-related emissions. B.  
11 Lejeune (private communication) has improved the OCS retrieval, with a better accuracy on  
12 seasonal amplitude, which is important for studying the carbon cycle and resolving temporal  
13 variability of OCS fluxes. Additionally, some sites measure in both NIR and MIR spectral  
14 regions, and therefore provide co-located and quasi-simultaneous CO<sub>2</sub> and OCS measurements.

15 The aim of this work is to exploit ground-based FTIR measurements of OCS to evaluate its  
16 sources and sinks, and further to use OCS as a tracer of photosynthesis. This is the first time  
17 using total/partial column data from FTIR networks to study the relationship  
18 between OCS and CO<sub>2</sub>. When interpreted by models, total column measurements are much less  
19 sensitive to assumptions on the boundary layer mixing, because every molecule in the  
20 atmospheric column is detected, independent of whether it is at the surface or in the upper  
21 troposphere. In order to obtain realistic fluxes by inverse models, assumptions must be made on  
22 the vertical mixing in the atmosphere, which is currently a large uncertainty in the transport  
23 of most models (Wunch et al., 2011; Yang et al., 2007; Keppel-Aleks et al., 2011). Therefore,  
24 column measurements of OCS and CO<sub>2</sub> could provide additional information for evaluating their  
25 terrestrial exchange.

26 In section 2, 3, and 4, we will describe the measurements, models, and inter-comparison between  
27 FTIR and model, respectively. In sections 5, we first analyze the FTIR measurements of OCS and  
28 CO<sub>2</sub> at selected sites. Then we compare OCS measurements to model simulations to evaluate the  
29 sources and sinks of OCS. Finally, we will discuss what can be learnt about CO<sub>2</sub> biospheric  
30 fluxes from OCS. The publication closes with the conclusion and outlook.

31

## 1 2. Measurements

### 2 2.1 FTIR

3 Five measurement sites are used in this study as a starting point for the research aim of using  
4 OCS to differentiate between photosynthetic and respiration fluxes of CO<sub>2</sub> (see details in Table 1).  
5 Ny-Ålesund and Bremen, which are operated by the University of Bremen, and Eureka, operated  
6 by the Canadian Network for the Detection of Atmospheric Change (CANDAC) and the  
7 University of Toronto, measure both OCS and CO<sub>2</sub>. The Jungfraujoch and Mauna Loa, operated  
8 by the University of Liège and National Center for Atmospheric Research (Hannigan et al., 2009),  
9 respectively, only measure in the MIR spectral region, and therefore TCCON-type CO<sub>2</sub> data are  
10 not available.

11 OCS profiles and total columns were retrieved using the SFIT-4 algorithm, based on the optimal  
12 estimation technique (Rodgers, 2000). A mixed spectroscopy based on the HITRAN 2012  
13 database was used in the retrievals. The a priori profile of OCS was provided by G. Toon (private  
14 communication), and modified according to the average tropopause height above each site  
15 (constant in the troposphere, and decrease above tropopause). Four spectral micro-windows were  
16 used in the fitting (B. Lejeune, private communication), containing the OCS v3 band P32, P28,  
17 P25, and P18 lines, respectively. Before fitting, spectra with a signal-to-noise ratio (SNR) of less  
18 than 100 were discarded. Post-fitting, retrievals with a root-mean-square (RMS) residual of  
19 greater than 0.5% were excluded before subsequent analysis. The retrieval parameters are  
20 summarized in Table 2.

21 To minimize the influence of the variations in stratosphere, the tropospheric partial columns were  
22 calculated from the surface to 9.8 km, based on the structure of the averaging kernels. In total,  
23 approximately 2.5 degrees of freedom for signal (DOFS) for total columns were obtained for all  
24 three sites. The DOFS for 0 to 9.8km is about 1. To make the values comparable to the in situ  
25 measurements, the tropospheric OCS column-averaged dry-air mole fractions (xOCS) were  
26 derived using Eq. (1):

$$27 \text{xOCS} = \text{Tropospheric OCS partial column} / \text{Tropospheric dry – air partial column} \quad (1)$$

28 The uncertainties are calculated using contributions from measurement uncertainties ( $S_m$ ), and  
29 forward model parameter uncertainties ( $S_f$ ) based on Rodgers (2000). The interference  
30 uncertainties ( $S_{\text{int}}$ ) are calculated as described by Rodgers and Connor (2003). The total

1 uncertainty in the tropospheric partial columns ( $S_{\text{total\_tropo}}$ ) was determined by adding these three  
2 components at each tropospheric layer (i) in quadrature:

$$3 \quad S_{\text{total\_tropo}} = \left( \sum_1^n (S_m(i)^2 + S_f(i)^2 + S_{\text{int}}(i)^2) \right)^{1/2} \quad (2)$$

4 The average uncertainties in the tropospheric partial columns from 2005 to 2012 are about 3% for  
5 all the sites.

6 The OCS retrievals from the FTIR spectra are not calibrated to account for biases due to the  
7 spectroscopy and other factors, therefore the means of the FTIR and in-situ measurements have  
8 an offset.

9 We use the GGG2012 version of the TCCON CO<sub>2</sub> data, available on <http://tccon.ornl.gov/2012>.  
10 CO<sub>2</sub> total columns as well as O<sub>2</sub> total columns were retrieved from near-infrared spectra using  
11 GFIT, following the TCCON standard procedure (Wunch et al., 2011). The CO<sub>2</sub> column is  
12 retrieved from two bands centered at 6228 cm<sup>-1</sup> and 6348 cm<sup>-1</sup>, while O<sub>2</sub> is retrieved from the  
13 electronic band centered at 7882 cm<sup>-1</sup>. CO<sub>2</sub> column-averaged dry-air mole fractions (DMF) were  
14 calculated by the following equation:

$$15 \quad xCO_2 = CO_2 / O_2 \times 0.2095 \quad (3)$$

## 16 **2.2 HIPPO**

17 The HIPPO (HIAPER Pole-to-Pole Observations) study of carbon cycle and greenhouse gases  
18 provides pole-to-pole measurements of meteorology, atmospheric chemistry, and aerosol content  
19 over the Pacific Ocean. HIPPO flew five month-long missions between January 2009 and  
20 September 2011 at different seasons. In this work, we use the NOAA flask sample data product  
21 of HIPPO (Wofsy et al., 2012), which provides additional information on the latitudinal  
22 distribution of the OCS and CO<sub>2</sub>. The OCS data (referred to as HIPPO-OCS) used in the work  
23 were measured by the NOAA “Whole Air Sampler-Montzka Mass Spectrometer #2” (NWAS-  
24 M2), while CO<sub>2</sub> concentrations (referred to as HIPPO-CO<sub>2</sub>) were measured by the NOAA  
25 “Whole Air Sampler-Measurement of Atmospheric Gases that Influence Climate Change”  
26 (NWAS-MAGICC).

27

## 28 **3. Model simulations**



### 1 **3.1 GEOS-Chem and CO<sub>2</sub> simulation**

2 The GEOS–Chem chemical transport model (version v9-01-03) is used in this study to simulate  
3 the concentrations of CO<sub>2</sub> and OCS in the global atmosphere. It is driven by assimilated  
4 meteorological observations from the Goddard Earth Observing System (GEOS) of the NASA  
5 Global Modeling Assimilation Office (GMAO) (Bey et al., 2001). The simulations were run  
6 using GEOS-5 meteorology from 2004 to 2012 on a horizontal grid resolution of 2 by 2.5 degrees  
7 (latitude by longitude), with 47 vertical levels. Taking 2004 as one year spin-up, we analyze the  
8 results from 2005 to 2012 based on hourly model output.

9 The CO<sub>2</sub> simulation module in GEOS-Chem was developed by Suntharalingam et al. (2003;  
10 2004), and updated by Nassar et al. (2010). The CO<sub>2</sub> fluxes used in GEOS-Chem version v9-01-  
11 03 include monthly fluxes of fossil fuel emissions from the Carbon Dioxide Information Analysis  
12 Center (CDIAC) inventory; biomass burning from the Global Fire Emission Database (GFED3);  
13 ocean exchange from Takahashi et al. (2009); and annual biofuel fluxes from Yevich and Logan  
14 (2003). GEOS-Chem uses CO<sub>2</sub> biospheric fluxes calculated from the Carnegie-Ames-Stanford-  
15 Approach (CASA; Olsen and Randerson, 2004) model for the year 2000 as a standard input, so  
16 that the biospheric fluxes do not have inter-annual variability. The CASA biospheric fluxes are  
17 balanced to zero at every grid, and therefore another terrestrial flux, which is referred to as the  
18 residual annual terrestrial exchange, is added to the simulation (Baker et al., 2006). In this study,  
19 we substitute the CASA biospheric fluxes with those calculated by the Simple Biosphere model  
20 (SiB; detail in section 3.3).

### 21 **3.2 OCS simulation**

22 The OCS module is developed from the version of Suntharalingam et al. (2008), and added to  
23 GEOS-Chem v9-01-03. It is largely based on the gridded flux inventories of Kettle et al. (2002a),  
24 hereafter referred to as K2002. The input fluxes from K2002 include ocean emissions,  
25 anthropogenic emissions, plant uptake, and soil uptake. The OCS biomass burning emission is  
26 calculated from CO emissions (from GFED3) using a scale factor from Nguyen et al. (1995). The  
27 tropospheric OH oxidation of OCS is calculated from OH monthly data (Park et al., 2004) and a  
28 temperature dependent rate (Atkinson et al., 1997). In addition, we included stratospheric loss  
29 (total loss from reaction with OH, O, and photolysis) in the OCS simulation to avoid the OCS  
30 accumulation above the troposphere. This stratospheric loss is computed using the altitude



1 dependent loss rate from Chin and Davis (1995). The OCS simulation with K2002 provides a  
2 baseline for evaluating the sources and sinks of OCS.

### 3 **3.3 The Simple Biosphere model (SiB)**

4 To study the relationship between OCS and CO<sub>2</sub>, we used the coupled fluxes from SiB. SiB was  
5 developed as a lower boundary for atmospheric models (Baker et al., 2013; Sellers et al., 1986),  
6 and has been coupled to General Circulation Models (GCMs; Sato et al., 1989; Randall et al.,  
7 1996) as well as mesoscale models (Denning et al., 2003; Nicholls et al., 2004; Wang et al., 2007;  
8 Corbin et al., 2008). Berry et al. (2013) incorporated the calculation of OCS uptake through  
9 stomata and in ground into SiB3 based on the biochemical mechanism for uptake of OCS by  
10 leaves and soils. This version of SiB is called SiB3-COS, and provides coupled simulations of  
11 CO<sub>2</sub> and OCS biospheric fluxes, including OCS plant uptake, OCS soil uptake, GPP, and CO<sub>2</sub>  
12 respiration. For this research, SiB3 simulations were performed on a 1.0 by 1.25 degree (latitude  
13 by longitude) grid, with meteorology provided by the Modern-Era Retrospective analysis for  
14 Research and Applications (MERRA; Reinecker et al., 2011). Precipitation fields were scaled to  
15 match Global Precipitation Climatology Project (GPCP; Adler et al., 2003) amplitudes globally.  
16 Respiration is scaled in SiB3, following Denning et al. (1996), to match productivity on a long-  
17 term basis; individual years are not in exact balance. Phenology (LAI, fPAR) is determined  
18 prognostically following Stöckli et al. (2008; 2011). Global GPP for the years 2000-2012  
19 averages 120 Gt C year<sup>-1</sup>, in reasonable agreement with flux tower-based estimates (Beer et al.,  
20 2010; Jung et al., 2011), although the spatiotemporal distribution of carbon uptake and efflux is  
21 uncertain.

22 In SiB, the OCS plant uptake is not scaled from GPP using a single factor, but estimated by  
23 mechanistic parameterization, consisting of several steps (Berry et al., 2013). OCS first diffuses  
24 from the boundary layer to the canopy, then from the canopy to the stomata, the stomata to the  
25 cells, and then is consumed in the cells. In the first step, the diffusion amount depends on the  
26 boundary layer concentration and diffusion conductance. The subsequent diffusion steps also  
27 depend on the conductance. The diffusion pathway of OCS is the same as that of CO<sub>2</sub>, but with  
28 different conductance. The consumption of OCS in the cells is by the enzyme carbonic anhydrase  
29 (CA), which is co-located with the enzyme that consumes CO<sub>2</sub> – Rubisco (Protoschill-Krebs and  
30 Kesselmeier, 1992; Protoschill-Krebs et al., 1996). CA activity and mesophyll conductance are

1 suggested to be proportional to the  $V_{\max}$  of Rubisco by some studies (Berry et al., 2013; Badger  
2 and Price, 1994; Evans et al., 1994), and this relationship is used in SiB to simulate the OCS  
3 uptake.

4 Soil uptake of OCS is a function of the activity of CA, as well as the condition of the soil (Berry  
5 et al., 2013; Van Diest and Kesselmeier, 2008). Due to the lack of information on soil CA activity,  
6 the soil uptake is instead calculated as a function of heterotrophic respiration (Rh), because  
7 measurements show that the OCS soil uptake is proportional to Rh (Yi et al., 2007). In Berry et al.  
8 (2013), the entire soil column was considered when scaling OCS soil uptake to Rh. Subsequent  
9 model versions have modified this treatment to consider only the top 20 cm of soil. Additionally,  
10  $J(\theta)$  (Equation 4, Berry et al., 2013) is no longer monotonically increasing from wet to dry soil,  
11 but rather follows a function (as Rh does in SiB) that peaks at an ‘optimum’ soil wetness based  
12 on soil character (Raich et al., 1991). Soil OCS uptake in SiB has been reduced from  
13 approximately one-half to around one-quarter of the uptake rate of the canopy, which is more in  
14 line with observations.

15 In this work, all the simulations were run using GEOS-Chem transport model. Two OCS land  
16 fluxes were used, K2002 and SiB, in the OCS simulations, summarized in Table 3. In the analysis,  
17 the simulations with different fluxes will be referred to as the fluxes names, as shown in Table 3.

18

#### 19 **4 Comparison between FTIR retrievals and model**

20 When comparing FTIR data with model simulations, the a priori and vertical sensitivity of the  
21 retrievals must be considered. We use the method described by Rodgers and Connor (2003). The  
22 hourly model vertical profiles were selected at the nearest grid point to the measurement sites and  
23 at measurement hours. The OCS profiles were smoothed by the FTIR a priori and averaging  
24 kernels of each measurement following the equation.

$$25 \quad X_s = X_a + A(X_m - X_a) \quad (4)$$

26 where  $X_s$ ,  $X_a$  and  $X_m$  are smoothed, a priori and model vertical profile, respectively, and A is the  
27 averaging kernel matrix. The tropospheric xOCS was then calculated using Eq. (1).

28 For  $\text{CO}_2$  column retrievals, Eq. (4) is modified (Wunch et al., 2010) to yield:

$$29 \quad C_s = C_a + h^T \times a^T \times (X_m - X_a) \quad (5)$$

1 where  $C_s$  and  $C_a$  are smoothed and a priori  $\text{CO}_2$  column-averaged DMF,  $h$  describes the vertical  
2 summation,  $a$  is the TCCON absorber-weighted column averaging kernel. TCCON averaging  
3 kernels are largely dependent on the solar zenith angle. Here we use the standard TCCON  
4 averaging kernel product, which provides the averaging kernels at five degree solar zenith angle  
5 intervals. The averaging kernels used here are interpolated to the solar zenith angle at the time the  
6 measurement was made.

7

## 8 **5 Results**

### 9 **5.1 The relationship between OCS and $\text{CO}_2$ in FTIR measurements**

10 Weekly mean calculated  $x\text{CO}_2$  and  $x\text{OCS}$  are shown in Figure 1. Both  $\text{CO}_2$  and OCS show clear  
11 seasonal variation with a maximum in late winter or early spring and a minimum in autumn. At  
12 Eureka, Ny-Ålesund and Bremen, OCS reaches its minimum about one month later than  $\text{CO}_2$ .  
13 The drawdown of  $\text{CO}_2$  results from the sum of the photosynthesis uptake and respiration  
14 emission. When respiration exceeds photosynthesis,  $\text{CO}_2$  starts increasing, while OCS is still  
15 decreasing due to the contribution of photosynthesis.

16 The FTIR measurements show a relative seasonal amplitude of OCS of about six times that of  
17  $\text{CO}_2$ , which is similar to the ratio derived from in-situ measurements (Montzka et al., 2007). The  
18 different magnitudes of the seasonal amplitudes are attributed to the absence of respiration, and to  
19 the leaf-scale relative uptake (LRU) rate of OCS to  $\text{CO}_2$ . Some laboratory and field experiments  
20 have shown that plants prefer OCS to  $\text{CO}_2$ , and obtained a LRU in the range of 1.3-5.5 for  
21 different species (Sandoval-Soto et al., 2005; Seibt et al., 2010; Stimler et al., 2010; Xu et al.,  
22 2002). If the LRU rate is known, the seasonal cycle of GPP can be determined from the OCS  
23 seasonal cycle, and measurements of OCS can be used to quantify GPP.

24 The seasonal amplitudes of both  $\text{CO}_2$  (approximately 3%) and OCS (approximately 17%) in Ny-  
25 Ålesund and Eureka are bigger than those in Bremen (approximately 2% and 12% for  $\text{CO}_2$  and  
26 OCS, respectively), Jungfrauoch (approximately 7% for OCS) and Mauna Loa (approximately 7%  
27 for OCS). This is caused by the effect of the boreal forest combined with advective transport. The  
28 photosynthesis in the boreal forest is strong during the polar day, leading to the rapid drawdown  
29 of both  $\text{CO}_2$  and OCS, which can be clearly seen in the measurements at the Arctic sites. For  
30 Jungfrauoch, the seasonal amplitude is smaller than that in Bremen, which partly results from its

1 high altitude, so that the variation in the lower atmosphere is not captured. Eliminating altitudes  
2 below 3.5km (the altitude of Jungfrauoch) from the calculation of xOCS at Ny-Ålesund and  
3 Bremen decreases their seasonal cycle amplitude by approximately 10%.

## 4 **5.2 OCS sources and sinks implied from FTIR measurements and model** 5 **comparisons**

### 6 **5.2.1 Simulation of OCS with K2002**

7 Prior to using the model relationship between OCS and CO<sub>2</sub>, we assess the accuracy of the OCS  
8 fluxes, starting with fluxes of K2002.

9 The simulations of OCS with K2002 are shown as blue asterisks in Figure 2. This simulation  
10 underestimates the seasonal amplitude, as reported by previous studies (Suntharalingam et al.,  
11 2008; Berry et al., 2013). Plant uptake is thought to be the dominant driver of seasonal variation  
12 in the Northern Hemisphere, so increasing the plant uptake should increase the seasonal  
13 amplitude. K2002 used a model based on Net Primary Production (NPP) to calculate the plant  
14 uptake of OCS, assuming the relative uptake rates for OCS and CO<sub>2</sub> were the same (Kettle et al.,  
15 2002a). That is,

$$16 \quad OCS \text{ uptake} = NPP \times [OCS]/[CO_2] \quad (6)$$

17 where [OCS] and [CO<sub>2</sub>] are the atmospheric concentrations of OCS and CO<sub>2</sub>, respectively. .  
18 Considering that OCS is taken up by plants irreversibly, while CO<sub>2</sub> is also released through  
19 respiration, and plants favor OCS over CO<sub>2</sub>, a model based on GPP has been suggested to replace  
20 the NPP-based model (Sandoval-Soto et al., 2005):

$$21 \quad OCS \text{ uptake} = GPP \times [OCS]/[CO_2] \times LRU \quad (7)$$

22 GPP is about two times as large as NPP, and the global averaged LRU is in the range of 1.3 – 3.1  
23 (Seibt et al., 2010; Stimler et al., 2012; Berkelhammer et al., 2014), so that in the GPP-based  
24 model, the OCS plant uptake is increased by a factor of 2.6 to 6.2 from the NPP model. Therefore  
25 the plant uptake in K2002 needs to be increased to match the seasonal cycle of the measurements.

26 Additionally, the simulation with K2002 underestimates the mean OCS value at Mauna Loa,  
27 implying a missing source at low latitudes. Berry et al. (2013) indicated that the missing source  
28 after increasing the land sinks is likely from the ocean, and distributed mainly in the tropical

1 region.

2 Following Suntharalingam et al. (2008), we rescaled the fluxes in K2002, including increasing  
3 the plant uptake, increasing the ocean emissions in the tropics, and decreasing the ocean  
4 emissions in the Southern Ocean, to find a better match to the column measurements. Multiplying  
5 the plant uptake by a factor of three (K2002x3, Figure 2. green stars) agrees with the  
6 measurements best.

## 7 **5.2.2 HIPPO latitudinal distribution**

8 To evaluate the latitudinal distribution of the fluxes, we compared the model simulations with  
9 HIPPO-OCS (Figure 3). To facilitate this comparison, the model mean was adjusted (by adding  
10 an offset of 30 ppt) to match the mean of the HIPPO measurements. The latitudinal distribution  
11 of the simulation with K2002 poorly matches the HIPPO-OCS. The K2002 simulation results in  
12 OCS concentrations that are too low in the tropics and too high in the Southern Hemisphere  
13 compared to the measurements from all five campaigns. In late northern summer (HIPPO-5) and  
14 autumn (HIPPO-2), the model is higher than the measurements in the boreal region, because the  
15 modeled plant uptake is too weak. After rescaling the plant uptake and ocean emissions, the  
16 latitudinal distribution of the simulation shows better agreement with HIPPO-OCS. However,  
17 there are still mismatches, especially in the tropical and northern temperate regions during  
18 HIPPO-2 and HIPPO-3, likely because sources in this region are too low in the model. This is  
19 also seen in Mauna Loa comparison between simulations and measurements. Increasing the  
20 ocean emissions in the Northern Hemisphere by a factor of two (not shown) results in a simulated  
21 increase in OCS in northern summer, at the time that ocean fluxes are greatest, while winter is  
22 hardly affected. Simply rescaling the fluxes based on the distribution (temporal and spatial) of  
23 K2002 is not sufficient to reproduce the latitudinal gradient of OCS: the seasonal cycles of the  
24 fluxes also need to be reconsidered. In this work, the ocean emissions were only modified at  
25 certain latitudes by a single regionally-specific factor. Because the role of ocean direct emissions  
26 is a subject of debate (Weiss et al., 1995; Xu et al., 2001; Berry et al., 2013; Launois et al., 2015a)  
27 and the temporal variations of the direct and indirect ocean emissions are similar (Kettle et al.,  
28 2002a), we take all ocean emissions as a whole when rescaling, similarly to the method in  
29 Suntharalingam et al. (2008). For the simulations with K2002x3 and SiB, a value of 0.5 was  
30 applied for the Southern Ocean (30° S - 90° S), while in the tropics (30° N - 30° S), values of 5.1  
31 and 5.2 were used for K2002x3 and SiB, respectively, to balance the global budget. Other studies

1 used atmospheric inversions (Berry et al., 2013; Kuai et al., 2015) or an ocean general circulation  
2 and biogeochemistry model (Launois et al., 2015a) to access the ocean fluxes, and gain better  
3 distribution. The global amount and general latitudinal distribution are consistent with this study.

4 The latitudinal gradient in the boreal region is more sensitive to plant uptake. Increasing plant  
5 uptake gives a steeper latitude gradient towards the Arctic. The simulation with K2002x3  
6 reproduced the strong gradient in summer and autumn, but the values are lower than the  
7 measurements - in agreement with the comparison with FTIR measurements. The mean values of  
8 the simulation with K2002x3 at the selected stations are lower than the FTIR measurements.

### 9 **5.3 Combination of OCS and CO<sub>2</sub> with SiB biospheric fluxes**

10 Although there are still uncertainties in the OCS sources and sinks, apart from land uptake and  
11 ocean emissions, their effect on the seasonal cycle in the northern high latitudes is small. Since  
12 we only increased the tropical ocean emissions, the ocean effect on the seasonal cycle in the  
13 northern high latitudes is smaller than that from land sinks. We used the coupled land fluxes of  
14 OCS and CO<sub>2</sub> from SiB to simultaneously simulate OCS and CO<sub>2</sub> with their seasonal cycles  
15 connected via the same modeled processes. Through the comparison of both species to the  
16 measurements, we can evaluate the GPP and Re in the biosphere model.

#### 17 **5.3.1 OCS simulation with SiB land fluxes**

18 The OCS simulation results with SiB fluxes are shown as magenta triangles in Figure 2. The  
19 mean values at the four high/mid latitude sites are higher than those with the original or rescaled  
20 K2002 fluxes, especially at Eureka and Ny-Ålesund. The simulated seasonal amplitudes with SiB  
21 fluxes at the selected sites are smaller than those simulated with K2002x3. From Table 3, shows  
22 that the plant uptake of SiB is about three times of K2002, and the soil uptake is also bigger than  
23 K2002. With identical distributions of these fluxes, one would expect a similar drawdown during  
24 growing season in the Northern Hemisphere from SiB compared to K2002x3. That this is not  
25 consistently present at the selected sites indicates that the latitudinal distribution of the land  
26 fluxes between SiB and Kettle is different.

27 We compared the difference between SiB and the scaled K2002 plant uptake and soil uptake in  
28 July, shown in Figure 4. For the plant uptake, SiB is much smaller than K2002x3 in the boreal  
29 forest region, causing a smaller drawdown, while it is stronger in the tropical region. Figure 5

1 (top) shows the monthly plant uptake of different fluxes summed globally, and in three latitude  
2 bands: 30°N to 90°N (North); 30°S to 30°N (Equatorial); and 90°S to 30°S (South). In the North  
3 region, the total amount and seasonal variation of the SiB plant uptake are smaller than K2002x3.  
4 The plant uptake of K2002 in the North region accounts for 42% of the global total uptake in a  
5 year, while for SiB plant uptake, it contributes only 24%. In Equatorial region the uptake in SiB  
6 is much larger than that in K2002x3. In the South, the plant uptake of SiB shows stronger  
7 seasonal variation than K2002x3. Globally, the SiB plant uptake is most consistent with K2002x3,  
8 though with a smaller seasonality, resulting from the strong uptake in the tropics and Southern  
9 Hemisphere. The difference in soil uptake between SiB and K2002 in July shows a similar  
10 pattern to the difference in plant uptake: larger uptake in the tropics and smaller uptake in the  
11 remaining regions. This latitudinal distribution of SiB OCS land fluxes leads to a higher mean  
12 value and smaller seasonal amplitude in the northern high latitudes, as seen from Eureka and Ny-  
13 Ålesund. The seasonal amplitude is better represented by SiB at the mid latitude site of  
14 Jungfrauoch.

15 Besides the seasonal amplitude, there are phase differences at Bremen and Jungfrauoch between  
16 the simulations with SiB fluxes and measurements. Due to the gap during polar winter, these  
17 cannot be evaluated at Eureka and Ny-Ålesund. The simulation with SiB shows higher values in  
18 the wintertime, which are also seen in the simulations with original and rescaled Kettle's flux.  
19 SiB, however, does not have a mechanism for OCS efflux, so the mean overestimation of OCS  
20 concentration in winter is by necessity a function of source location/magnitude and/or transport.  
21 The simulation with SiB fluxes reaches the minimum earlier than the measurements. If we  
22 discount transport errors, this indicates that there is more OCS uptake (either from plants or soils)  
23 in the real world than that calculated in the model in the autumn. The minimum offset is not seen  
24 in the simulations with K2002x3, and the seasonal variations of plant uptake are similar in SiB  
25 and K2002x3 in the Northern Hemisphere (Figure 5, top), so the early minimum in SiB may  
26 result from the smaller soil uptake in autumn compared to K2002, which is shown in Figure 5  
27 (bottom). As mentioned in section 3.3, the soil uptake used in this work is smaller than that in  
28 Berry et al. (2013). This could mean that the actual soil uptake is stronger or continues longer.  
29 However, the temporal and spatial pattern of K2002 fluxes is with large uncertainties: the plant  
30 uptake is estimated from the NPP-base model; the soil uptake is calculated using an empirical  
31 algorithm with the parameterization determined for one arable soil type only, which is a likely  
32 source of error (Kettle et al., 2002a). Therefore, the early minimum in SiB cannot be attributed to



1 soil uptake through the comparison to K2002. Further investigation is needed to understand the  
2 minimum shift.

3 The comparison between the SiB simulation and HIPPO-OCS measurements is shown in  
4 magenta lines in Figure 3. The simulation with SiB fluxes results in a lower value in the Southern  
5 Hemisphere than the rescaled Kettle fluxes. This matches the HIPPO-OCS better, because SiB  
6 has a stronger plant uptake in the tropics and Southern Hemisphere. For the Northern Hemisphere,  
7 the low OCS concentrations in the low and mid latitudes (HIPPO-2, HIPPO-3) are due to a  
8 combination of sources and/or transport, as are the simulations with Kettle's fluxes. SiB did not  
9 capture the strong latitudinal gradient during growing season (HIPPO-5), indicating the plant  
10 uptake of OCS in SiB in the boreal forest is too small, at least for the year (2011) in question.

### 11 **5.3.2 Implications for CO<sub>2</sub> fluxes in SiB from OCS comparison**

12 We hope to gain additional information on the CO<sub>2</sub> biospheric fluxes with the help of OCS. Since  
13 the CO<sub>2</sub> and OCS uptake by photosynthesis is coupled in SiB, one can calculate the GPP using  
14 the OCS uptake amount. This evaluation is complicated, however, because OCS and CO<sub>2</sub> go  
15 through the diffusion and consumption steps independently in SiB. The LRU is a diagnostic  
16 quantity that comes out of the simulations following explicit calculation of CO<sub>2</sub> and OCS fluxes.  
17 LRU varies by vegetation type, season, and time of day with uncertainties. However, these fluxes  
18 can still be evaluated by combining the comparison of OCS and CO<sub>2</sub> between simulations and  
19 measurements.

20 As discussed in section 5.3.1, SiB underestimated the OCS drawdown at Eureka and Ny-Ålesund,  
21 and poorly represented the latitudinal gradient in the Northern Hemisphere. This indicates that  
22 the photosynthetic uptake could be underestimated in northern high latitudes. We examine this  
23 further by comparing the CO<sub>2</sub> simulations with measurements.

24 The simulation of CO<sub>2</sub> with SiB fluxes represents the seasonal cycles at all the three sites well  
25 (Figure 6, left panels), unlike with the OCS comparison. From the mean seasonal cycles (Figure 6,  
26 right panels) the minima in the CO<sub>2</sub> seasonal cycles are later in the simulation than measurements,  
27 indicating that the increase of CO<sub>2</sub> after the growing season is slower in the model. We also  
28 compared the CO<sub>2</sub> latitudinal distribution between HIPPO-CO<sub>2</sub> and model simulations (Figure 7).  
29 The difference in the Southern Hemisphere between the HIPPO-CO<sub>2</sub> and model is very small, so  
30 the main disagreement is in the northern high latitudes. In late autumn (HIPPO-2), SiB gives

1 lower values than the HIPPO data in the boreal region. This supports the late minimum in  
2 comparison to the FTIR measurements. In spring (HIPPO-3), the simulation is higher than the  
3 HIPPO measurements in the Arctic. Previous studies showed that SiB3 performed well in the  
4 forest region of North America (Schwalm et al., 2010), while did a poor job in some Arctic  
5 tundra regions, caused by an over-sensitivity to very low temperature (Fisher et al., 2014). During  
6 the northern growing season, the SiB simulation of CO<sub>2</sub> resulted in a strong latitudinal gradient,  
7 which matches the HIPPO measurements well (HIPPO-5), illustrating that the net CO<sub>2</sub> fluxes  
8 have a reasonable latitudinal distribution, unlike with the OCS simulation.

9 The seasonal cycle of OCS is mainly influenced by the plant uptake, which is connected with  
10 GPP, while CO<sub>2</sub> seasonality results from the sum of both GPP and Re. Huntzinger et al. (2012)  
11 have shown that models can get similar NEP with gross fluxes (GPP and Re) that differ by a  
12 factor of two or more. If OCS plant uptake is used as a proxy for GPP and the LRU is reasonable,  
13 one can infer that the GPP estimated in SiB is low in the northern boreal region, which cannot be  
14 seen in the CO<sub>2</sub> simulation driven by NEP, meaning that the Re in SiB must also be low, so that  
15 the weak uptake is cancelled out in the net flux. However, the LRU is still uncertain. If LRU is  
16 low in general in the Northern Hemisphere, a reasonable GPP estimate could occur together with  
17 a small OCS uptake. Therefore the relationship of OCS and CO<sub>2</sub> in SiB needs to be further  
18 verified. However, these results indicate that while the NEP is reasonably modeled, its individual  
19 component fluxes might be in error. This inference is made possible through the combination of  
20 OCS and CO<sub>2</sub> measurements.

21 The early minimum in SiB simulation of OCS compared to the measurements is indicative of  
22 weak uptake in the autumn. If this is caused by an weak OCS plant uptake, CO<sub>2</sub> assimilation  
23 would also be small, leading to a shorter period of CO<sub>2</sub> drawdown in the simulation, which is the  
24 opposite of what is shown in Figure 6. Therefore, it is more likely that OCS soil uptake is too  
25 small in SiB in the autumn. Because the OCS soil uptake in SiB is proportional to Rh, the  
26 respiration could also be too small. This would explain the late minimum in the CO<sub>2</sub> simulation.  
27 Another possibility is that the LRU becomes very large in the autumn, so the OCS uptake is still  
28 strong while CO<sub>2</sub> decreases to a very small value. Experiments have shown that the LRU  
29 increases under low light condition (Stimler et al., 2010). We do not have sufficient information  
30 at this time to determine the most likely reason for SiB to show a shift in the seasonal cycle  
31 minimum between the OCS simulation and the measurements. However, the combination of OCS

1 and CO<sub>2</sub> atmospheric measurements opens some new avenues to explore how the biospheric  
2 models reproduce the carbon cycle in the real world.

3

## 4 **6 Conclusions**

5 For the first time, FTIR measurements of OCS and CO<sub>2</sub> were used to study their relationship.  
6 OCS retrieved from FTIR spectra at the five sites showed clear seasonal cycles, and confirmed  
7 the similarity to CO<sub>2</sub> variations.

8 We compared the OCS column measurements to simulations with original and rescaled versions  
9 of fluxes based on Kettle et al. (2002a). The results indicate that increasing the plant uptake and  
10 ocean emissions improves the comparison. The OCS simulations were also compared to HIPPO  
11 in-situ measurements. Increasing plant uptake leads to a stronger latitudinal gradient in the  
12 Northern Hemisphere during growing season and better agreement with HIPPO-OCS. However,  
13 the latitudinal distribution of the rescaled fluxes mismatches the HIPPO-OCS measurements in  
14 the tropical and northern temperate zone, implying a missing source in that region. Further  
15 studies are needed to optimize the OCS sources and sinks.

16 Simulations using coupled SiB land fluxes of CO<sub>2</sub> and OCS show good agreement of CO<sub>2</sub> with  
17 FTIR measurements at selected sites, but underestimated OCS drawdown. Through the  
18 comparison with HIPPO-OCS measurements, a weaker gradient in the Northern Hemisphere  
19 during growing season can be seen in the simulation. Using OCS as a GPP proxy, the GPP  
20 estimation in the Northern Hemisphere could be low in SiB. However, the relationship between  
21 OCS plant uptake and GPP in the model needs to be further verified.

22 The seasonal cycle minimum offset between simulation and measurements is not consistent for  
23 OCS and CO<sub>2</sub>. The simulation presents an early minimum for OCS but a late minimum for CO<sub>2</sub>  
24 when compared to the measurements. These phase differences offer another aspect that can be  
25 used to evaluate the photosynthesis and respiration in SiB. Several possibilities which could  
26 cause this inconsistency have been discussed, but further research is needed before reaching a  
27 conclusion. Looking at OCS and CO<sub>2</sub> together inspires some new thoughts in how the biospheric  
28 models reproduce the carbon cycle in the real world.

29

## 30 **7 Outlook**

1 This work will be extended to more sites, including some in the Southern Hemisphere, to  
2 evaluate the seasonal cycles of OCS and CO<sub>2</sub> in different regions. The FTIR networks will  
3 provide an additional database for using OCS to constraint GPP, which would be further  
4 improved if more frequency, simultaneous measurements of OCS and CO<sub>2</sub> where available at a  
5 greater number of sites.

6 Using coupled OCS and CO<sub>2</sub> land fluxes in a biospheric model and comparing to measurements  
7 of both gases provides the method to constrain GPP with the help of OCS. The relationship  
8 between OCS and CO<sub>2</sub> uptake in SiB can be further verified by field measurements for more  
9 plant types and at different time. This will increase the confidence for making conclusions on  
10 GPP distribution and time variation from the view of OCS.

11 Although the relationship between OCS plant uptake and GPP still has uncertainties, OCS could  
12 be used to study the biospheric processes driving the inter-annual variability. Some climate  
13 extremes have impacts on both photosynthesis and respiration; for instance, high temperature  
14 could decrease photosynthetic production and increase respiration. With the help of OCS, these  
15 biospheric feedbacks could be distinguished.

16

## 17 **Acknowledgements:**

18 This work is partly supported by the DFG, project PA 1714/6-1. Nicholas Deutscher is supported  
19 by an Australian Research Council – Discovery Early Career Researcher Award, DE140100178.  
20 We thank the AWI for support in carrying out the measurements in Ny-Ålesund, Spitsbergen.  
21 The University of Liège contribution to the present work has primarily been supported by the  
22 A3C and ACROSAT PRODEX projects (Belgian Science Policy Office, BELSPO, Brussels).  
23 The Liege team further acknowledges crucial support by MeteoSwiss (GAW-CH), the F.R.S. –  
24 FNRS and the Fédération Wallonie-Bruxelles. We thank the International Foundation High  
25 Altitude Research Stations Jungfrauoch and Gornergrat (HFSJG, Bern). The National Center for  
26 Atmospheric Research is supported by the National Science Foundation. The NCAR FTS  
27 observation program at Mauna Loa, HI is supported under contract by the National Aeronautics  
28 and Space Administration (NASA). We wish to thank NOAA for support of the MLO station.  
29 The Eureka measurements were made at the Polar Environment Atmospheric Research  
30 Laboratory (PEARL) by the Canadian Network for the Detection of Atmospheric Change

1 (CANDAC), led by James R. Drummond, and in part by the Canadian Arctic ACE Validation  
2 Campaigns, led by Kaley A. Walker. They were supported by the AIF/NSRIT, CFI, CFCAS,  
3 CSA, EC, GOC-IPY, NSERC, NSTP, OIT, PCSP, and ORF. Additionally, we thank Steve Wofsy  
4 and all other HIPPO members for making the HIPPO and NOAA data available to the public  
5 from the HIPPO website at <http://hippo.ornl.gov/>.

6

## 7 **References**

8 Adler, A. F., Huffman, G. J., Chang, A., Ferraro, R., Xie, P.-P., Janowiak, J., Rudolf, B.,  
9 Schneider, U., Curtis, S., Bolvin, D., Gruber, A., Susskind, J., Arkin, P., and Nelkin, E.: The  
10 Version-2 Global Precipitation Climatology Project (GPCP) Monthly Precipitation Analysis  
11 (1979–Present), *J. Hydrometeorol.*, 4, 1147–1167, 2003.

12 Atkinson, R., Baulch, D. L., Cox, R. A., Hampson Jr., R. F., Kerr, J. A., Rossi, J. M., and Troe J.:  
13 Evaluated kinetic, photochemical and heterogeneous data for atmospheric chemistry, *J. Phys.*  
14 *Chem. Ref. Data*, 26, 521-1011, 1997.

15 Badger, M. R., and Price G. D.: The role of carbonic-anhydrase in photosynthesis, *Annu. Rev.*  
16 *Plant Phys.*, 45, 369-392, 1994.

17 Baker, D. F., Law, R. M., Gurney, K. R., Rayner, P., Peylin, P., Denning, A. S., Bousquet, P.,  
18 Bruhwiler, L., Chen, Y.-H., Ciais, P., Fung, I. Y., Heimann, M., John, J., Maki, T., Maksyutov, S.,  
19 Masarie, K., Prather, M., Pak, B., Taguchi, S., and Zhu, Z.: TransCom 3 inversion  
20 intercomparison: Impact of transport model errors on the interannual variability of regional CO<sub>2</sub>  
21 fluxes, 1988–2003, *Global Biogeochem. Cy.*, 20, GB1002, doi:10.1029/2004GB002439, 2006.

22 Baker, I. T., Harper, A. B., da Rocha, H. R., Denning, A. S., Araújo, A. C., Borma, L. S., Freitas,  
23 H. C., Goulden, M. L., Manzi, A. O., Miller, S. D., Nobre, A. D., Restrepo-Coupe, N., Saleska, S.  
24 R., Stöckli, R., von Randow, C., and Wofsy, S. C.: Surface ecophysiological behavior across  
25 vegetation and moisture gradients in tropical South America, *Agr. Forest Meteorol.*, 182, 177-188,  
26 doi:10.1016/j.agrformet.2012.11.015, 2013.

27 Barkley, M. P., Palmer, P. I., Boone, C. D., Bernath, P. F., and Suntharalingam, P.: Global  
28 distributions of carbonyl sulfide in the upper troposphere and stratosphere, *Geophys. Res.*  
29 *Lett.*, 35, L14810, doi:10.1029/2008GL034270, 2008. Barthlott, S., Schneider, M., Hase, F.,  
30 Wiegele, A., Christner, E., Gonzalez, Y., Blumenstock, T., Dohe, S., Garcia, O., Sepúlveda, E.,

1 Strong, K., Mendonca, J., Weaver, D., Palm, M., Deutscher, N. M., Warneke, T., Notholt, J.,  
2 Lejeune, B., Mahieu, E., Jones, N., Griffith, D. W. T., Velasco, V. A., Smale, D., Robinson, J.,  
3 Kivi, R., Heikkinen, P., and Raffalski, U.: Using XCO<sub>2</sub> retrievals for assessing the long-term  
4 consistency of NDACC/FTIR data sets, *Atmos. Meas. Tech.*, 8, 1555-1573, doi:10.5194/amt-8-  
5 1555-2015, 2015.

6 Beer, C., Reichstein, M., Tomelleri, E., Ciais, P., Jung, M., Carvalhais, N., Rödenbeck, C., Arain,  
7 M. A., Baldocchi, D., Bonan, G. B., Bondeau, A., Cescatti, A., Lasslop, G., Lindroth, A., Lomas,  
8 M., Luyssaert, S., Margolis, H., Oleson, K. W., Rouspard, O., Veenendaal, E., Viovy, N.,  
9 Williams, C., Woodward, F. I., and Papale, D.: Terrestrial gross carbon dioxide uptake: Global  
10 Distribution and covariation with climate, *Science*, 329, 834-838, doi:10.1126/science.1184984,  
11 2010.

12 Belviso, S., Schmidt, M., Yver, C., Ramonet, M., Gros, V., and Launois, T.: Strong similarities  
13 between nighttime deposition velocities of carbonyl sulphide and molecular hydrogen inferred  
14 from semi-continuous atmospheric observations in Gif-sur-Yvette, Paris region, *Tellus B*, 65,  
15 20719, doi:10.3402/tellusb.v65i0.20719, 2013.

16 Berkelhammer, M., Asaf, D., Still, C., Montzka, S., Noone, D., Gupta, M., Provencal, R., Chen,  
17 H., and Yakir, D.: Constraining surface carbon fluxes using in situ measurements of carbonyl  
18 sulfide and carbon dioxide, *Global Biogeochem. Cy.*, 28, 161-179, doi:10.1002/2013GB004644,  
19 2014.

20 Berry, J., Wolf, A., Campbell, J. E., Baker, I., Blake, N., Blake, D., Denning, A. S., Kawa, S. R.,  
21 Montzka, S. A., Seibt, U., Stimler, K., Yakir, D., and Zhu, Z.: A coupled model of the global  
22 cycles of carbonyl sulfide and CO<sub>2</sub>: a possible new window on the carbon cycle, *J. Geophys.*  
23 *Res.-Biogeo.*, 118, 842-852, 2013.

24 Bey, I., Jacob, D. J., Yantosca, R. M., Logan, J. A., Field, B. D., Fiore, A. M., Li, Q., Liu, H. Y.,  
25 Mickley, L. J., and Schultz, M. G.: Global modeling of tropospheric chemistry with assimilated  
26 meteorology: Model description and evaluation, *J. Geophys. Res.-Atmos.*, 106, 23073-23095,  
27 doi:10.1029/2001JD000807, 2001.

28 Buschmann, M., Deutscher, N. M., Sherlock, V., Palm, M., Warneke, T., and Notholt, J.:  
29 Retrieval of xCO<sub>2</sub> from ground-based mid-infrared (NDACC) solar absorption spectra and  
30 comparison to TCCON, *Atmos. Meas. Tech.*, in review, 2015.

1 Campbell, J. E., Carmichael, G. R., Chai, T., Mena-Carrasco, M., Tang, Y., Blake, D. R., Vay, S.  
2 A., Collatz, G. J., Baker, I., Berry, J. A., Montzka, S. A., Sweney, C., Schnoor, J. L., and Stanier,  
3 C. O.: Photosynthetic control of atmospheric carbonyl sulfide during the growing season, *Science*,  
4 322, 1085-1088, 2008.

5 Campbell, J. E., Whelan, M. E., Seibt, U., Smith, S. J., Berry, J. A., and Hilton, T. W.:  
6 Atmospheric carbonyl sulfide sources from anthropogenic activity: Implications for carbon cycle  
7 constraints, *Geophys. Res. Lett.*, 42, 3004-3010, 2015.

8 Cheng, Y., Zhang, C., Zhang, Y., Zhang, H., Sun, X., and Mu, Y.: Characteristics and  
9 anthropogenic sources of carbonyl sulfide in Beijing, *J. Environ. Sci.*, 28, 163-170,  
10 doi:10.1016/j.jes.2014.05.052, 2015.

11 Chin, M., and Davis, D. D.: A reanalysis of carbonyl sulfide as a source of stratospheric  
12 background sulfur aerosol. *J. Geophys. Res.*, 100(D5):8993–9005, 1995.

13 Corbin, K. D., Denning, A. S., Lu, L., Wang, J.-W., and Baker, I. T.: Possible representation  
14 errors in inversions of satellite CO<sub>2</sub> retrievals, *J. Geophys. Res.*, 113, D2,  
15 doi:10.1029/2007JD008716, 2008.

16 Denning, A. S., Collatz, G. J., Zhang, C., Randall, D. A., Berry, J. A., Sellers, P. J., Colello, G.  
17 D., and Dazlich, D. A.: Simulation of terrestrial carbon metabolism and atmospheric CO<sub>2</sub> in a  
18 general circulation model. Part I: Surface carbon fluxes, *Tellus B*, 48, 521-542, 1996.

19 Denning, A. S., Nicholls, M., Prihodko, L., Baker, I., Vidale, P.-L., Davis, K., and Bakwin, P.:  
20 Simulated variations in atmospheric CO<sub>2</sub> over a Wisconsin forest using a coupled ecosystem–  
21 atmosphere model, *Glob. Change Biol.*, 9, 1241-1250, 2003.

22 Evans, J. R., Caemmerer, S. V., Setchell, B. A., and Hudson, G. S.: The relationship between  
23 CO<sub>2</sub> transfer conductance and leaf anatomy in transgenic tobacco with a reduced content of  
24 Rubisco, *Aust. J. Plant Physiol.*, 21, 475-495, 1994.

25 Fisher, J. B., Sikka, M., Oechel, W. C., Huntzinger, D. N., Melton, J. R., Koven, C. D., Ahlström,  
26 A., Arain, M. A., Baker, I., Chen, J. M., Ciais, P., Davidson, C., Dietze, M., El-Masri, B., Hayes,  
27 D., Huntingford, C., Jain, A. K., Levy, P. E., Lomas, M. R., Poulter, B., Price, D., Sahoo, A. K.,  
28 Schaefer, K., Tian, H., Tomelleri, E., Verbeeck, H., Viovy, N., Wania, R., Zeng, N., and Miller,  
29 C. E.: Carbon cycle uncertainty in the Alaskan Arctic, *Biogeosciences*, 11, 4271-4288,  
30 doi:10.5194/bg-11-4271-2014, 2014.



1 Glatthor, N., Höpfner, M., Baker, I. T., Berry, J., Campbell, J. E., Kawa, S. R., Krysztofiak, G.,  
2 Leyser, A., Sinnhuber B.-M., and Stinecipher, J.: Tropical sources and sinks of carbonyl sulfide  
3 observed from space, *Geophys. Res. Lett.*, 42, 10082-10090, doi: 10.1002/2015GL066293,  
4 2015. Goldan, P. D., Fall, R., Kuster, W. C., and Fehsenfeld, F. C.: Uptake of COS by growing  
5 vegetation: A major tropospheric sink, *J. Geophys. Res.*, 93, D11, 14186-14192, 1988.

6 Guo, H., Simpson, I. J., Ding, A. J., Wang, T., Saunders, S. M., Wang, T. J., Cheng, H. R.,  
7 Barletta, B., Meinardi, S., Blake, D. R., and Rowland, F. S.: Carbonyl sulfide, dimethyl sulfide  
8 and carbon disulfide in the Pearl River Delta of southern China: Impact of anthropogenic and  
9 biogenic sources. *Atmos. Environ.*, 44, 31, 3805-3813, doi:10.1016/j.atmosenv.2010.06.040,  
10 2010.

11 Hannigan, J.W., Coffey, M.T., and Goldman, A.: Semiautonomous FTS Observation System for  
12 Remote Sensing of Stratospheric and Tropospheric Gases, *J. Atmos. Oceanic Technol.*, 26, 1814–  
13 1828. doi: 10.1175/2009JTECHA1230.1, 2009.

14 Huntzinger, D., Post, W., Michelak, A., Wei, Y., Jacobsen, A., West, T. O., Baker, I., Chen, J.,  
15 Davis, K., Hayes, D., Hoffman, F., Jain, A., Liu, S., McGuire, D., Neilson, R., Poulter, B., Tian,  
16 H., Thornton, P., Tomelleri, E., Viovy, N., Xiao, J., Zeng, N., Zhao, M., and Cook, R.: North  
17 American Carbon Project (NACP) regional interim synthesis: terrestrial biospheric model  
18 intercomparison, *Ecol. Model.*, 232, 144-157, doi:10.1016/j.ecolmodel.2012.02.004, 2012.

19 Jung, M., Reichstein, M., Margolis, H. A., Cescatti, A., Richardson, A. D., Arain, M. A., Arneth,  
20 A., Bernhofer, C., Bonal, D., Chen, J., Gianelle, D., Gobron, N., Kiely, G., Kutsch, W., Lasslop,  
21 G., Law, B. E., Lindroth, A., Merbold, L., Montagnani, L., Moors, E. J., Papale, D., Sottocornola,  
22 M., Vaccari, F., and Williams, C.: Global patterns of land-atmosphere fluxes of carbon dioxide,  
23 latent heat, and sensible heat derived from eddy covariance, satellite, and meteorological  
24 observations, *J. Geophys. Res.*, 116, G00J07, doi:10.1029/2010JG001566, 2011.

25 Keppel-Aleks, G., Wennberg, P. O., and Schneider, T.: Sources of variations in total column  
26 carbon dioxide, *Atmos. Chem. Phys.*, 11, 3581-3593, doi:10.5194/acp-11-3581-2011, 2011.

27 Kettle, A. J., Kuhn, U., von Hobe, M., Kesselmeier, J., and Andreae, M. O.: Global budget of  
28 atmospheric carbonyl sulfide: temporal and spatial variations of the dominant sources and sinks, *J.*  
29 *Geophys. Res.-Atmos.*, 107, 4658, doi:10.1029/2002JD002187, 2002a.

30 Kettle, A. J., Kuhn, U., von Hobe, M., Kesselmeier, J., Liss, P. S., and Andreae, M. O.: Comparin

1 g forward and inverse models to estimate the seasonal variation of hemisphere-integrated fluxes  
2 of carbonyl sulfide, *Atmos. Chem. Phys.*, 2, 343-361, 2002b.

3 Kuai, L., Worden, J., Kulawik, S. S., Montzka, S. A., and Liu, J.: Characterization of aura  
4 tropospheric emissions spectrometer carbonyl sulfide retrievals over ocean, *Atmos. Meas. Tech.*,  
5 7, 163–172, doi:10.5194/amt-7-163-2014, 2014.

6 Kuai, L., Worden, J. R., Campbell, J. E., Kulawik, S. S., Lee, M., Weidner, R. J., Li, K., Montzka,  
7 S. A., Moore, F. L., Berry, J.A., Baker, I., Denning, S., Bian, H., Bowman, K., Liu, J., and Yung,  
8 Y.: Estimate of Carbonyl Sulfide Tropical Oceanic Surface Fluxes Using Aura Tropospheric  
9 Emission Spectrometer Observations, *J. Geophys. Res.-Atmos.*, accepted,  
10 doi:10.1002/2015JD023493, 2015.

11 Launois, T., Belviso, S., Bopp, L., Fichot, C. G., and Peylin, P.: A new model for the global  
12 biogeochemical cycle of carbonyl sulfide – Part 1: Assessment of direct marine emissions with an  
13 oceanic general circulation and biogeochemistry model, *Atmos. Chem. Phys.*, 15, 2295-2312,  
14 2015a.

15 Launois, T., Peylin, P., Belviso, S., and Poulter, B.: A new model of the global biogeochemical  
16 cycle of carbonyl sulfide – Part 2: Use of carbonyl sulfide to constrain gross primary productivity  
17 in current vegetation models, *Atmos. Chem. Phys.*, 15, 9285-9312, doi:10.5194/acp-15-9285-  
18 2015, 2015. Montzka, S. A., Calvert, P., Hall, B. D., Elkins, J. W., Conway, T. J., Tans, P. P., and  
19 Sweeney, C.: On the global distribution, seasonality, and budget of atmospheric carbonyl sulfide  
20 (COS) and some similarities to CO<sub>2</sub>, *J. Geophys. Res.-Atmos.*, 112, D09302,  
21 doi:10.1029/2006JD007665, 2007.

22 Nassar, R., Jones, D. B. A., Suntharalingam, P., Chen, J. M., Andres, R. J., Wecht, K. J.,  
23 Yantosca, R. M., Kulawik, S. S., Bowman, K. W., Worden, J. R., Machida T., and Matsueda H.:  
24 Modeling global atmospheric CO<sub>2</sub> with improved emission inventories and CO<sub>2</sub> production from  
25 the oxidation of other carbon species, *Geoscientific Model Development*, 3, 689-716, 2010.

26 Nguyen, B. C., Mihalopoulos, N., Putaud, J. P., and Bonsang, B.: Carbonyl sulfide emissions  
27 from biomass burning in the tropics, *J. Atmos. Chem.*, 22, 55-65, 1995.

28 Nicholls, M. E., Denning, A. S., Prihodko, L., Vidale, P.-L., Baker, I., Davis, K., and Bakwin, P.:  
29 A multiple-scale simulation of variations in atmospheric carbon dioxide using a coupled  
30 biosphere–atmosphere model, *J. Geophys. Res.*, 109, D18, doi:10.1029/2003JD004482, 2004.

1 Notholt, J., Kuang, Z., Rinsland, C. P., Toon, G. C., Rex, M., Jones, N., Albrecht, T.,  
2 Deckelmann, H., Krieg, J., Weinzierl, C., Bingemer, H., Weller, R., and Schrems, O.: Enhanced  
3 upper tropical tropospheric COS: Impact on the stratospheric aerosol layer, *Science*, 300, 5617,  
4 307-310, doi: 10.1126/science.1080320, 2003.Olsen, S. C., and Randerson, J. T.: Differences  
5 between surface and column atmospheric CO<sub>2</sub> and implications for carbon cycle research, *J.*  
6 *Geophys. Res.*, 109, D02301, doi:10.1029/2003JD003968, 2004.

7 Park, R. J., Jacob, D. J., Field, B. D., Yantosca, R. M., and Chin, M.: Natural and transboundary  
8 pollution influences on sulfate-nitrate-ammonium aerosols in the United States: Implications for  
9 policy, *J. Geophys. Res.*, 109, D15204, doi:10.1029/2003JD004473, 2004.

10 Protoschill-Krebs, G. and Kesselmeier, J.: Enzymatic pathways for the consumption of carbonyl  
11 sulphide (COS) by higher plants, *Bot. Acta*, 105, 206–212, doi:10.1111/j.1438-  
12 8677.1992.tb00288.x, 1992.

13 Protoschill-Krebs, G., Wilhelm, C., and Kesselmeier, J.: Consumption of carbonyl sulphide (COS)  
14 by higher plant carbonic anhydrase (CA), *Atmos. Environ.*, 30, 18, 3151–3156,  
15 doi:10.1016/1352-2310(96)00026-X, 1996.Raich, J. W., Rastetter, E. B., Melillo, J. M.,  
16 Kicklighter, D. W., Steudler, P. A., Peterson, B. J., Grace, A. L., Moore III, B., and Vorosmarty,  
17 C. J.: Potential Net Primary Productivity in South America: Application of a Global Model, *Ecol.*  
18 *Appl.*, 1, 399-429, 1991.

19 Randall, D. A., Dazlich, D. A., Zhang, C., Denning, A. S., Sellers, P. J., Tucker, C. J., Bounoua,  
20 L., Berry, J. A., Collatz, G. J., Field, C. B., Los, S. O., Justice, C. O., and Fung, I.: A revised land  
21 surface parameterization (SiB2) for GCMs. Part III: the greening of the Colorado State  
22 University General Circulation Model, *J. Climate*, 9, 738-763, 1996.

23 Rienecker, M. M., Suarez, M. J., Gelaro, R., Todling, R., Bacmeister, J., Liu, E., Bosilovich, M.  
24 G., Schubert, S. D., Takacs, L., Kim, G.-K., Bloom, S., Chen, J., Collins, D., Conaty, A., da Silva,  
25 A., Gu, W., Joiner, J., Koster, R. D., Lucchesi, R., Molod, A., Owens, T., Pawson, S., Pegion, P.,  
26 Redder, C. R., Reichle, R., Robertson, F. R., Ruddick, A. G., Sienkiewicz, M., and Woollen, J.:  
27 MERRA: NASA's Modern-Era Retrospective Analysis for Research and Applications, *J.*  
28 *Climate*, 24, 3624–3648, 2011.

29 Rodgers, C. D., *Inverse Methods for Atmospheric Sounding: Theory and Practice*, Series  
30 *Atmospheric, Oceanic and Planetary Physics*, vol.2, 238pp., World Scientific, Singapore, 2000.

1 Rodgers, C. D. and Connor, B. J.: Intercomparison of remote sounding instruments, *J. Geophys.*  
2 *Res.*, 108, 4116, doi:10.1029/2002JD002299, 2003.

3 Sandoval-Soto, L., Stanimirov, M., von Hobe, M., Schmitt, V., Valdes, J., Wild, A., and  
4 Kesselmeier, J.: Global uptake of carbonyl sulfide (COS) by terrestrial vegetation: Estimates  
5 corrected by deposition velocities normalized to the uptake of carbon dioxide (CO<sub>2</sub>),  
6 *Biogeosciences*, 2, 125-132, doi:10.5194/bg-2-125-2005, 2005.

7 Sato, N., Sellers, P. J., Randall, D. A., Schneider, E. K., Shukla, J., Kinter, J. L., Hou, Y-T., and  
8 Albertazzi, E.: Effects of implementing the Simple Biosphere Model in a General Circulation  
9 Model, *J. Atmos. Sci.*, 46, 2757-2782, 1989.

10 Schwalm, C. R., Williams, C. A., Schaefer, K., Anderson, R., Arain, M. A., Baker, I., Barr, A.,  
11 Black, T. A., Chen, G. S., Chen, J. M., Ciais, P., Davis, K. J., Desai, A., Dietze, M., Dragoni, D.,  
12 Fischer, M. L., Flanagan, L. B., Grant, R., Gu, L. H., Hollinger, D., Izaurrealde, R. C., Kucharik,  
13 C., Lafleur, P., Law, B. E., Li, L. H., Li, Z. P., Liu, S. G., Lokupitiya, E., Luo, Y. Q., Ma, S. Y.,  
14 Margolis, H., Matamala, R., McCaughey, H., Monson, R. K., Oechel, W. C., Peng, C. H., Poulter,  
15 B., Price, D. T., Riciutto, D. M., Riley, W., Sahoo, A. K., Sprintsin, M., Sun, J. F., Tian, H. Q.,  
16 Tonitto, C., Verbeeck, H., and Verma, S. B.: A model-data intercomparison of CO<sub>2</sub> exchange  
17 across North America: Results from the North American Carbon Program site synthesis, *J.*  
18 *Geophys. Res.-Biogeo.*, 115, G00H05, doi:10.1029/2009JG001229, 2010.

19 Sellers, P. J., Mintz, Y., Sud, Y. C., and Dalcher A.: A simple biosphere model (SIB) for use  
20 within general-circulation models, *J. Atmos. Sci.*, 43, 505-531, 1986.

21 Seibt, U., Kesselmeier, J., Sandoval-Soto, L., Kuhn, U., and Berry, J. A.: A kinetic analysis of  
22 leaf uptake of COS and its relation to transpiration, photosynthesis and carbon isotope  
23 fractionation, *Biogeosciences*, 7, 333-341, doi:10.5194/bg-7-333-2010, 2010.

24 Steinbacher, M., Bingemer, H. G., and Schmidt, U.: Measurements of the exchange of carbonyl  
25 sulfide (OCS) and carbon disulfide (CS<sub>2</sub>) between soil and atmosphere in a spruce forest in  
26 central Germany. *Atmos. Environ.*, 38, 35, 6043-6052, doi:10.1016/j.atmosenv.2004.06.022,  
27 2004. Stimler, K., Montzka, S. A., Berry, J. A., Rudich, Y., and Yakir, D.: Relationships between  
28 car-bonyl sulfide (COS) and CO<sub>2</sub> during leaf gas exchange, *New Phytol.*, 186, 869-878, 2010.

29 Stimler, K., Berry, J. A., and Yakir, D.: Effects of carbonyl sulfide and carbonic anhydrase on  
30 stomatal conductance, *Plant Physiol.*, 158, 524-530, 2012.

1 Stöckli, R., Rutishauser, T., Dragoni, D., O'Keefe, J., Thornton, P. E., Jolly, M., Lu, L., Denning,  
2 A. S.: Remote sensing data assimilation for a prognostic phenology model, *J. Geophys. Res.-*  
3 *Biogeo.*, 113, G04021, doi:10.1029/2008JG000781, 2008.

4 Stöckli, R., Rutishauser, T., Baker, I., Körner, C., Liniger, M. A., and Denning, A. S.: A Global  
5 Reanalysis of Vegetation Phenology, *J. Geophys. Res.-Biogeo.*, 116, G03020,  
6 doi:10.1029/2010JG001545, 2011.

7 Sun, W., Maseyk, K., Lett, C., and Seibt, U.: A soil diffusion–reaction model for surface COS  
8 flux: COSSM v1, *Geosci. Model Dev.*, 8, 3055-3070, doi:10.5194/gmd-8-3055-2015,  
9 2015.Suntharalingam, P., Spivakovsky, C. M., Logan, J. A., and McElroy, M. B.: Estimating the  
10 distribution of terrestrial CO<sub>2</sub> sources and sinks from atmospheric measurements: Sensitivity to  
11 configuration of the observation network, *J. Geophys. Res.*, 108, 4452,  
12 doi:10.1029/2002JD002207, 2003.

13 Suntharalingam, P., Jacob, D. J., Palmer, P. I., Logan, J. A., Yantosca, R. M., Xiao, Y., Evans, M.  
14 J., Streets, D. G., Vay, S. L., and Sachse, G. W.: Improved quantification of Chinese carbon  
15 fluxes using CO<sub>2</sub>/CO correlations in Asian outflow, *J. Geophys. Res.*, 109, D18S18,  
16 doi:10.1029/2003JD004362, 2004.

17 Suntharalingam, P., Kettle, A. J., Montzka, S. M., and Jacob, D. J.: Global 3-D model analysis of  
18 the seasonal cycle of atmospheric carbonyl sulfide: implications for terrestrial vegetation uptake,  
19 *Geophys. Res. Lett.*, 35, L19801, doi:10.1029/2008GL034332, 2008.

20 Takahashi, T., Sutherland, S. C., Wanninkhof, R., Sweeney, C., Feely, R. A., Chipman, D. W.,  
21 Hales, B., Friederich, G., Chavez, F., Sabine, C., Watson, A., Bakker, D. C. E., Schuster, U.,  
22 Metzl, N., Yoshikawa-Inoue, H., Ishii, M., Midorikawa, T., Nojiri, Y., Körtzinger, A., Steinhoff,  
23 T., Hoppema, M., Olafsson, J., Arnarson, T. S., Tilbrook, B., Johannessen, T., Olsen, A.,  
24 Bellerby, R., Wong, C. S., Delille, B., Bates, N. R., and de Baar, H. J. W.: Climatological mean  
25 and decadal change in surface ocean pCO<sub>2</sub>, and net sea-air CO<sub>2</sub> flux over the global oceans,  
26 *Deep Sea Research Part II: Topical Studies in Oceanography*, 56, 554-577,  
27 doi:10.1016/j.dsr2.2008.12.009, 2009.

28 Van Diest, H., and Kesselmeier J.: Soil atmosphere exchange of carbonyl sulfide (COS) regulated  
29 by diffusivity depending on water-filled pore space, *Biogeosciences*, 5, 475-483, 2008.

30 Wang, J. W., Denning, A. S., Lu, L., Baker, I. T., Corbin, K. D., and Davis, K. J.: Observations

1 and simulations of synoptic, regional, and local variations in atmospheric CO<sub>2</sub>, *J. Geophys. Res.*,  
2 112, D0418, doi:10.1029/2006JD007410, 2007.

3 Weiss, P. S., Johnson, J. E., Gammon, R. H., and Bates, T. S.: Reevaluation of the open ocean  
4 source of carbonyl sulfide to the atmosphere, *J. Geophys. Res.-Atmos*, 100, D11, 23083-23092,  
5 doi:10.1029/95JD01926, 1995. Whelan, M. E., Min, D. H., and Rhew, R. C.: Salt marsh  
6 vegetation as a carbonyl sulfide (COS) source to the atmosphere, *Atmos. Environ.*, 73, 131-137,  
7 2013.

8 Wofsy, S. C., Daube, B. C., Jimenez, R., Kort, E., Pittman, J. V., Park, S., Commane, R., Xiang,  
9 B., Santoni, G., Jacob, D., Fisher, J., Pickett-Heaps, C., Wang, H., Wecht, K., Wang, Q.-Q.,  
10 Stephens, B. B., Shertz, S., Watt, A. S., Romashkin, P., Campos, T., Haggerty, J., Cooper, W. A.,  
11 Rogers, D., Beaton, S., Hendershot, R., Elkins, J. W., Fahey, D. W., Gao, R. S., Moore, F.,  
12 Montzka, S. A., Schwarz, J. P., Perring, A. E., Hurst, D., Miller, B. R., Sweeney, C., Oltmans, S.,  
13 Nance, D., Hintsa, E., Dutton, G., Watts, L. A., Spackman, J. R., Rosenlof, K. H., Ray, E. A.,  
14 Hall, B., Zondlo, M. A., Diao, M., Keeling, R., Bent, J., Atlas, E. L., Lueb, R., and Mahoney, M.  
15 J.: HIPPO NOAA Flask Sample GHG, Halocarbon, and Hydrocarbon Data (R\_20121129),  
16 Carbon Dioxide Information Analysis Center, Oak Ridge National Laboratory, Oak Ridge,  
17 Tennessee, U.S.A. [http://dx.doi.org/10.3334/CDIAC/hippo\\_013](http://dx.doi.org/10.3334/CDIAC/hippo_013) (Release 20121129), 2012.

18 Wunch, D., Toon, G. C., Wennberg, P. O., Wofsy, S. C., Stephens, B. B., Fischer, M. L., Uchino,  
19 O., Abshire, J. B., Bernath, P., Biraud, S. C., Blavier, J.-F. L., Boone, C., Bowman, K. P.,  
20 Browell, E. V., Campos, T., Connor, B. J., Daube, B. C., Deutscher, N. M., Diao, M., Elkins, J.  
21 W., Gerbig, C., Gottlieb, E., Griffith, D. W. T., Hurst, D. F., Jiménez, R., Keppel-Aleks, G., Kort,  
22 E. A., Macatangay, R., Machida, T., Matsueda, H., Moore, F., Morino, I., Park, S., Robinson, J.,  
23 Roehl, C. M., Sawa, Y., Sherlock, V., Sweeney, C., Tanaka, T., and Zondlo, M. A.: Calibration  
24 of the Total Carbon Column Observing Network using aircraft profile data, *Atmos. Meas. Tech.*,  
25 3, 1351-1362, doi:10.5194/amt3-1351-2010, 2010.

26 Wunch, D., Toon, G. C., Blavier, J.-F. L., Washenfelder, R. A., Notholt, J., Connor, B. J., Griffith,  
27 D. W. T., Sherlock, V., and Wennberg, P. O.: The Total Carbon Column Observing Network,  
28 *Philos. T. R. Soc. A*, 369, 2087-2112, doi:10.1098/rsta.2010.0240, 2011.

29 Xu, X., Bingemer, H. G., Georgii, H. W., Schmidt, U., and Bartell, U.: Measurements of carbonyl  
30 sulfide (COS) in surface seawater and marine air, and estimates of the air-sea flux from

1 observations during two Atlantic cruises, *J. Geophys. Res.-Atmos.*, 106, D4, 3491–3502,  
2 doi:10.1029/2000JD900571, 2001.

3 Xu, X., Bingemer, H. G., and Schmidt, U.: The flux of carbonyl sulfide and carbon disulfide  
4 between the atmosphere and a spruce forest, *Atmos. Chem. Phys.*, 2, 171-181, doi:10.5194/acp-2-  
5 171-2002, 2002. Yang, Z., Washenfelder, R. A., Keppel-Aleks, G., Krakauer, N. Y., Randerson, J.  
6 T., Tans, P. P., Sweeney, C., and Wennberg, P. O.: New constraints on Northern Hemisphere  
7 growing season net flux, *Geophys. Res. Lett.*, 34, L12807, doi:10.1029/2007GL029742, 2007.

8 Yevich, R., and Logan, J. A.: An assessment of biofuel use and burning of agricultural waste in  
9 the developing world, *Global Biogeochem. Cy.*, 17, 1095, doi:10.1029/2002GB001952, 2003.

10 Yi, Z. G., Wang, X. M., Sheng, G. Y., Zhang, D. Q., Zhou, G. Y., and Fu, J. M.: Soil uptake of  
11 carbonyl sulfide in subtropical forests with different successional stages in south China, *J.*  
12 *Geophys. Res.*, 112, D08302, doi:10.1029/2006JD008048, 2007.

13  
14  
15  
16  
17  
18  
19  
20  
21  
22  
23  
24  
25  
26  
27



1 Table 1. FTIR sites used in this study

Site	Latitude (°N)	Longitude (°E)	Altitude (m a.s. l.)	Instrument	Measurement years	Network
Eureka	80.1	-86.4	610	Bomem DA8 125HR	1993-2008 2006-present	NDACC& TCCON
Ny-Ålesund	78.9	11.9	21	120HR 120-5HR	1992-2012 2013-present	NDACC& TCCON
Bremen	53.1	8.8	27	120HR 125HR	2002-2003 2004-present	NDACC& TCCON
Jungfraujoch	46.5	8.0	3580	homemade 120HR	1984-2008 1990-present	NDACC
Mauna Loa	19.5	-155.6	3397	Bomem DA8 120HR 125HR	1991-1995 1995-2011 2011-present	NDACC

2  
3  
4  
5  
6  
7  
8  
9  
10

1 Table 2. Summary of the retrieval parameters for OCS

Retrieval code	Spectroscopy	A priori profiles	OCS	A priori matrix	S <sub>a</sub>	Microwindows (cm <sup>-1</sup> )	Interfering species	SNR	Pressure, Temperature profiles
SFIT4_v0.9.4	Based on HITRAN 2012	Provided by G. Toon over private communication, modified by tropopause height		In-situ measurement variability below 9 km, ACE-FTS measurement variability above 9 km		2047.78-2048.22 2049.75-2050.12 2051.18-2051.48 2054.33-2054.67	O <sub>3</sub> , H <sub>2</sub> O, CO, H <sub>2</sub> <sup>18</sup> O, <sup>13</sup> CO <sub>2</sub> , <sup>18</sup> OCO	300 (pre-fixed)	NCEP

2  
3  
4  
5  
6  
7  
8  
9  
10  
11  
12  
13  
14  
15  
16  
17

1 Table 3. Annual global atmospheric OCS budget (fluxes in Gg S year<sup>-1</sup>)

	K2002 <sup>a</sup>	K2002x3	SiB
	Mean (Range)	Revisions	Revisions
<i>Sources</i>			
Anthropogenic	182 (90-266)		
Ocean	280 (39-520)	754	757
Biomass burning	35 (25-38) <sup>b</sup>		
<i>Sinks</i>			
Plant	238 (210-270)	713	688
Soil	130 (74-180)		159
Tropospheric OH oxidation	96 (95-98) <sup>b</sup>		
Stratosphere loss	28 <sup>b</sup>		
Net	5	4	3

2 <sup>a</sup> Modifications include biomass burning, tropospheric OH oxidation, and stratospheric loss. (see  
3 text)

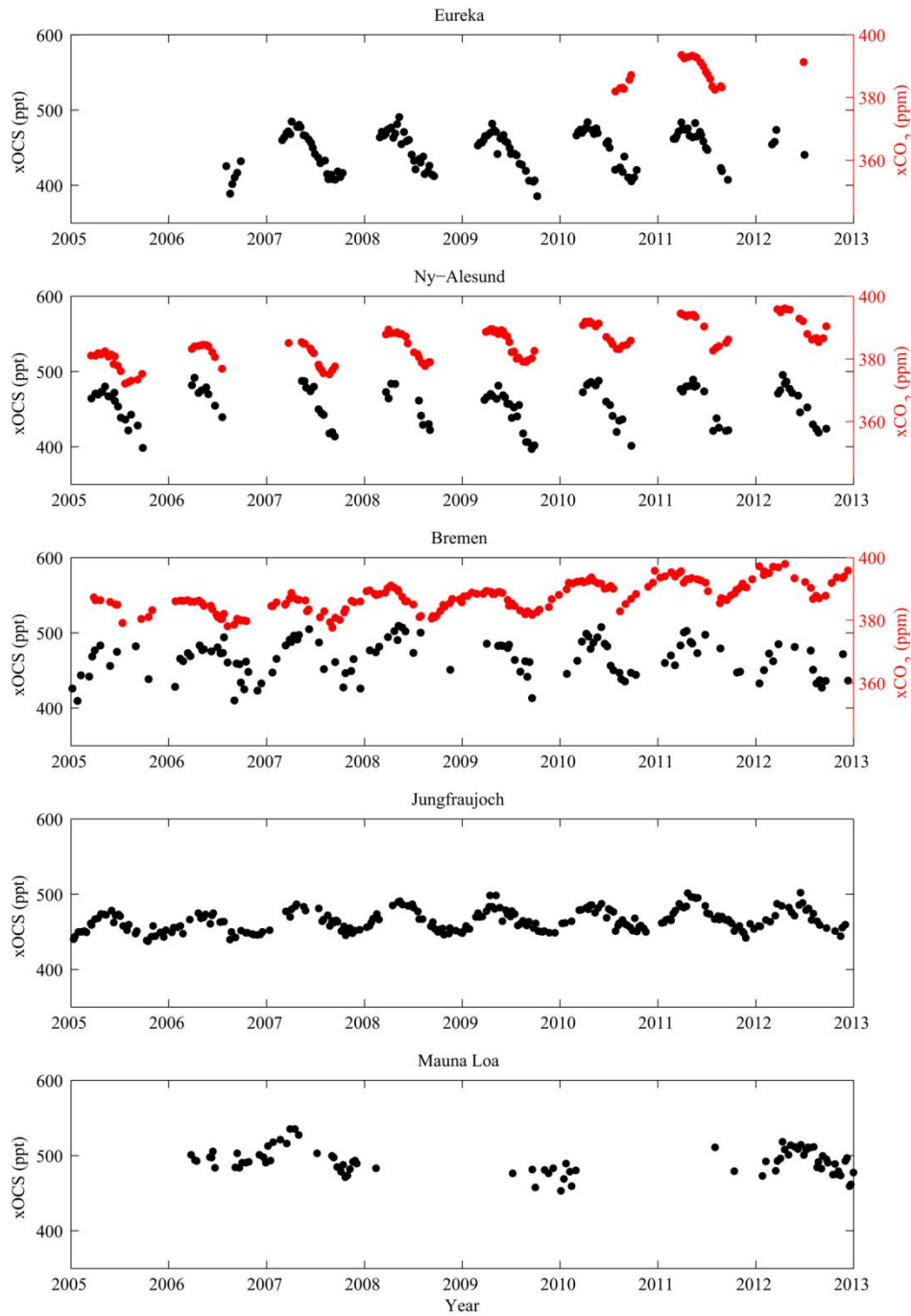
4 <sup>b</sup> The range for biomass burning and tropospheric OH oxidation is the range calculated in the  
5 model from 2005 to 2012; the calculated stratospheric loss varies little.

6

7

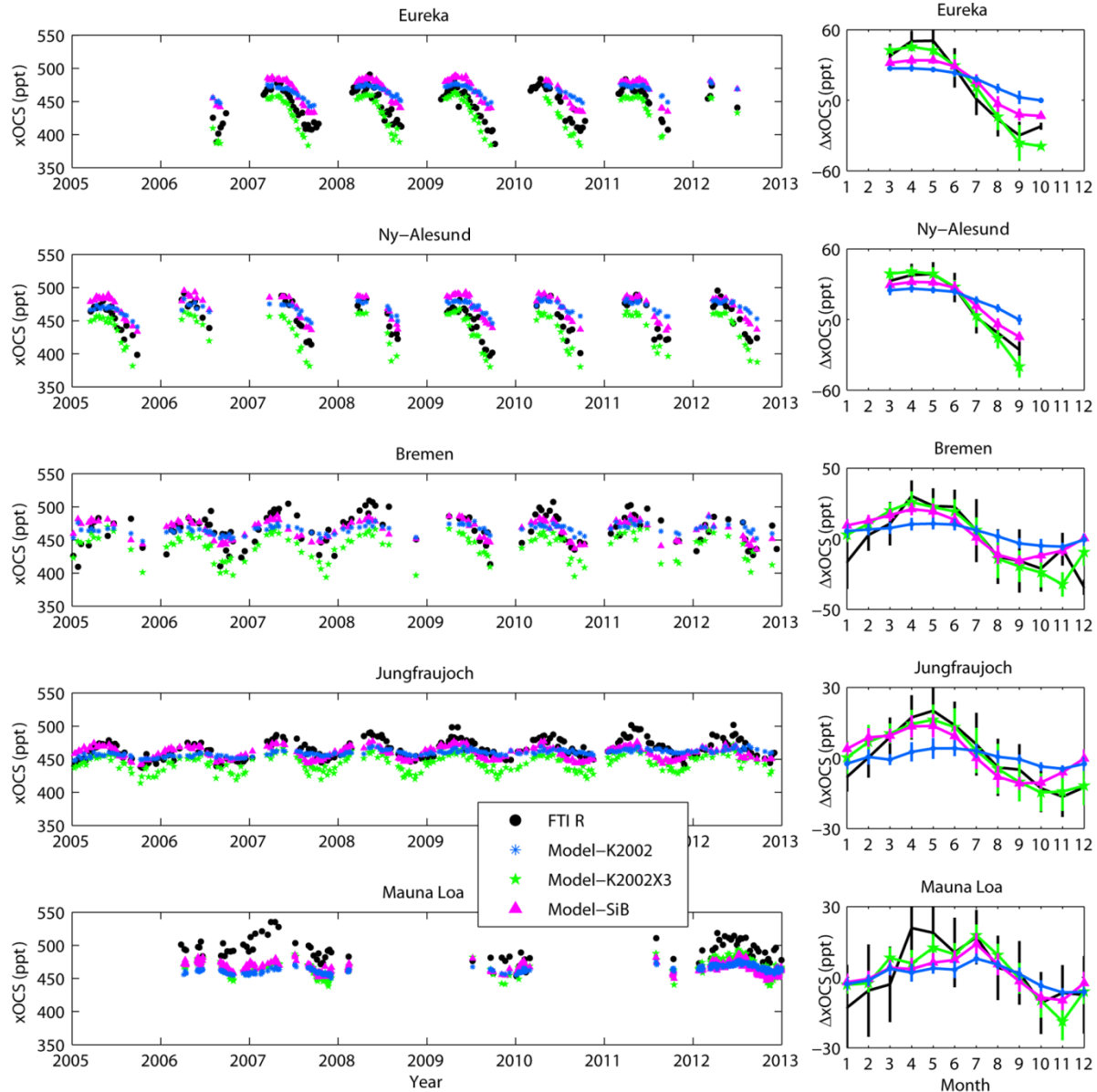
8

9



1  
 2 Figure 1. Weekly mean xOCS (black dots) and xCO<sub>2</sub> (red dots) retrieved from FTIR spectra at  
 3 Eureka, Ny Ålesund, Bremen, Jungfrauoch and Mauna Loa.

4

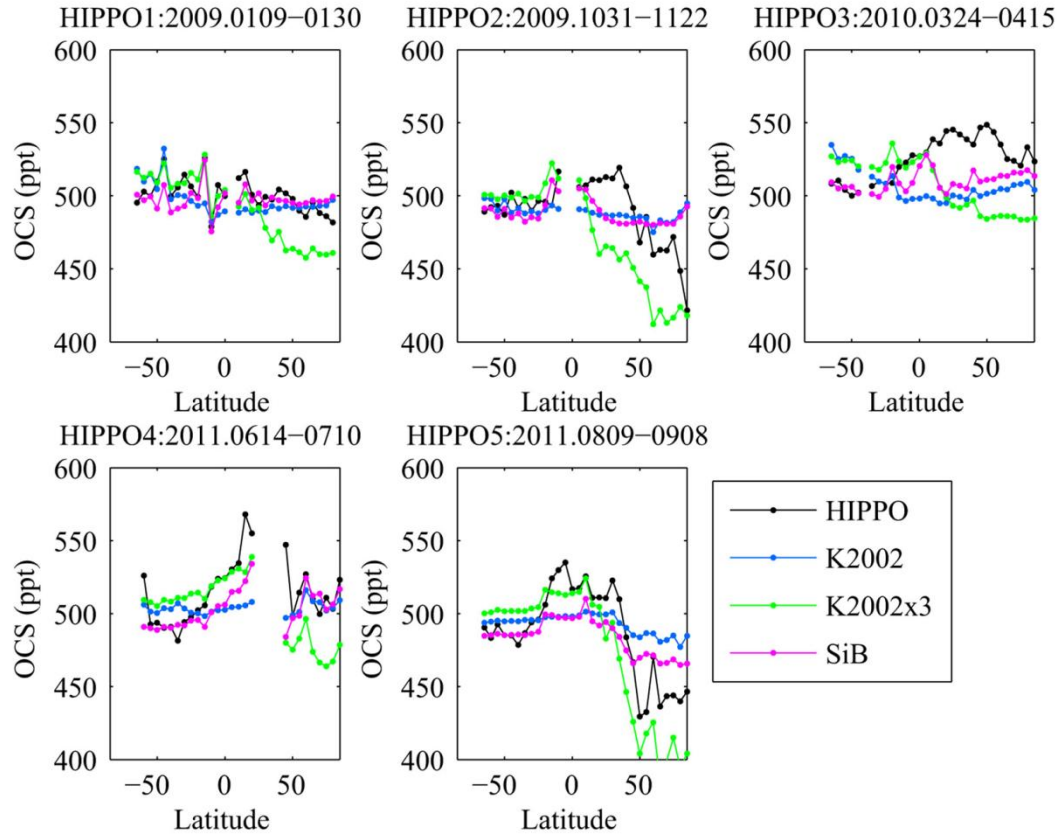


1  
 2 Figure 2. Comparison of FTIR measurements of OCS to model simulations at Eureka, Ny-  
 3 Ålesund, Bremen, Jungfraujoch and Mauna Loa. The left panels show weekly means from 2005  
 4 to 2012. The right panels are the monthly mean relative xOCS (relative to annual mean) averaged  
 5 for multiple years. The error bars are the standard deviations of each month. The FTIR retrievals  
 6 are shown in black dots. The model simulations are driven by K2002 (blue asterisks), K2002x3  
 7 (green stars), and SiB (magenta triangles).

8

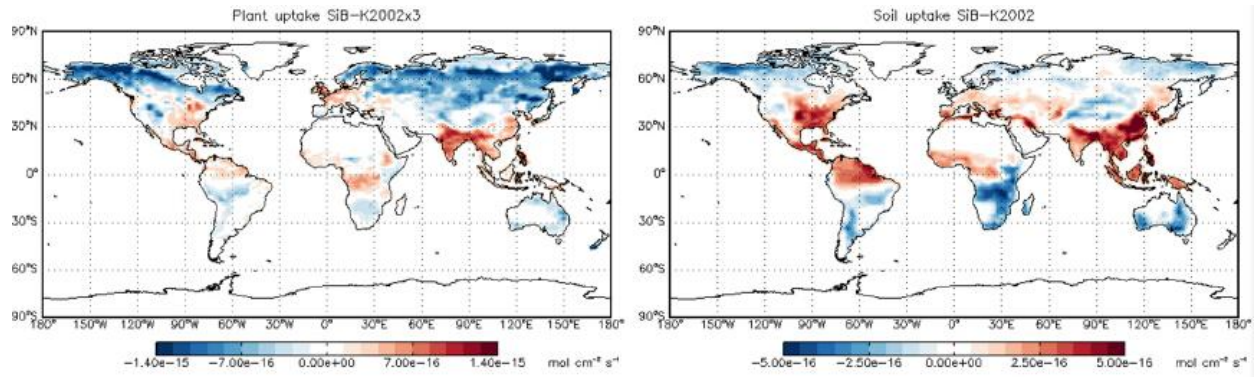
9

10



1  
 2 Figure 3. Comparison of HIPPO OCS measurements and model simulations. The five campaigns  
 3 are compared separately to show latitudinal gradient at different seasons. To minimize the  
 4 influence of the stratosphere, only the measurements lower than 9 km are used. The model  
 5 outputs are selected at the nearest measurement location and time. The measurements and model  
 6 output are averaged in five degree bins. The HIPPO data are shown in black dots. The model  
 7 simulations are in the same colors with those shown in Figure 2.

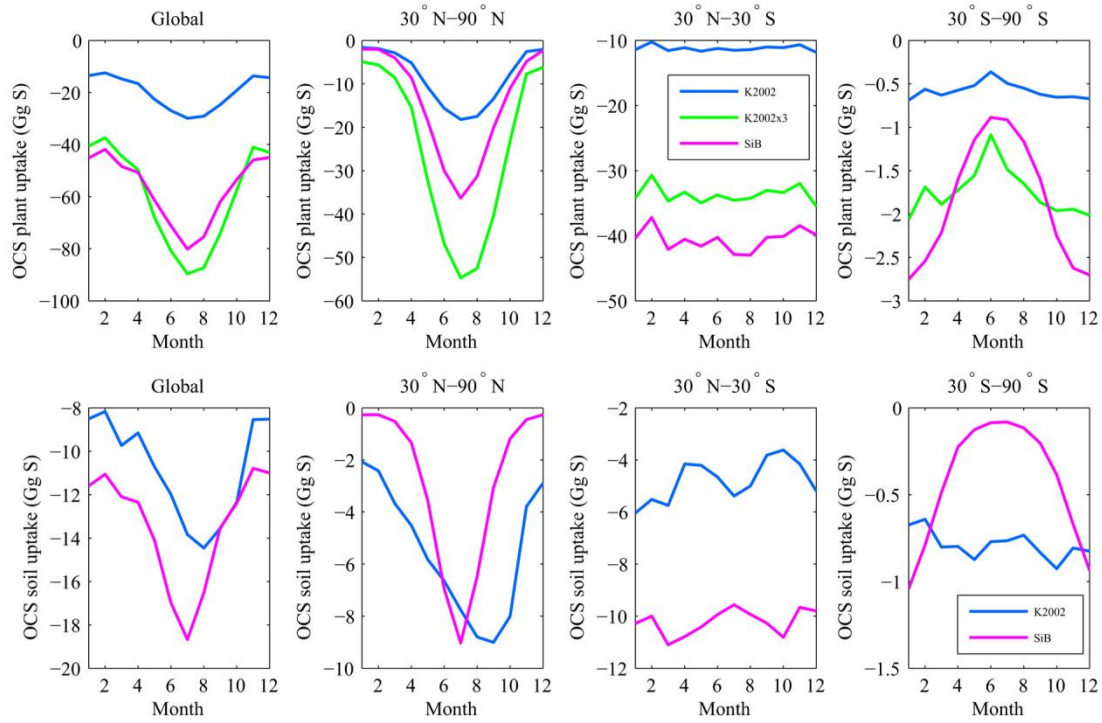
8  
 9  
 10  
 11  
 12  
 13



1  
2  
3  
4  
5  
6  
7  
8  
9  
10  
11  
12  
13  
14  
15  
16  
17  
18  
19  
20  
21

Figure 4. Difference between SiB OCS plant uptake and K2002x3 (left, SiB – K2002x3), difference between OCS soil uptake and K2002 (right, SiB – K2002)





1  
 2 Figure 5. Monthly totals of OCS plant uptake (top) and soil uptake (bottom) of K2002 (blue),  
 3 K2002x3 (green), and SiB (magenta) for global, 30° N - 90° N, 30°N - 30° S, and 30° S - 90° S.

4

5

6

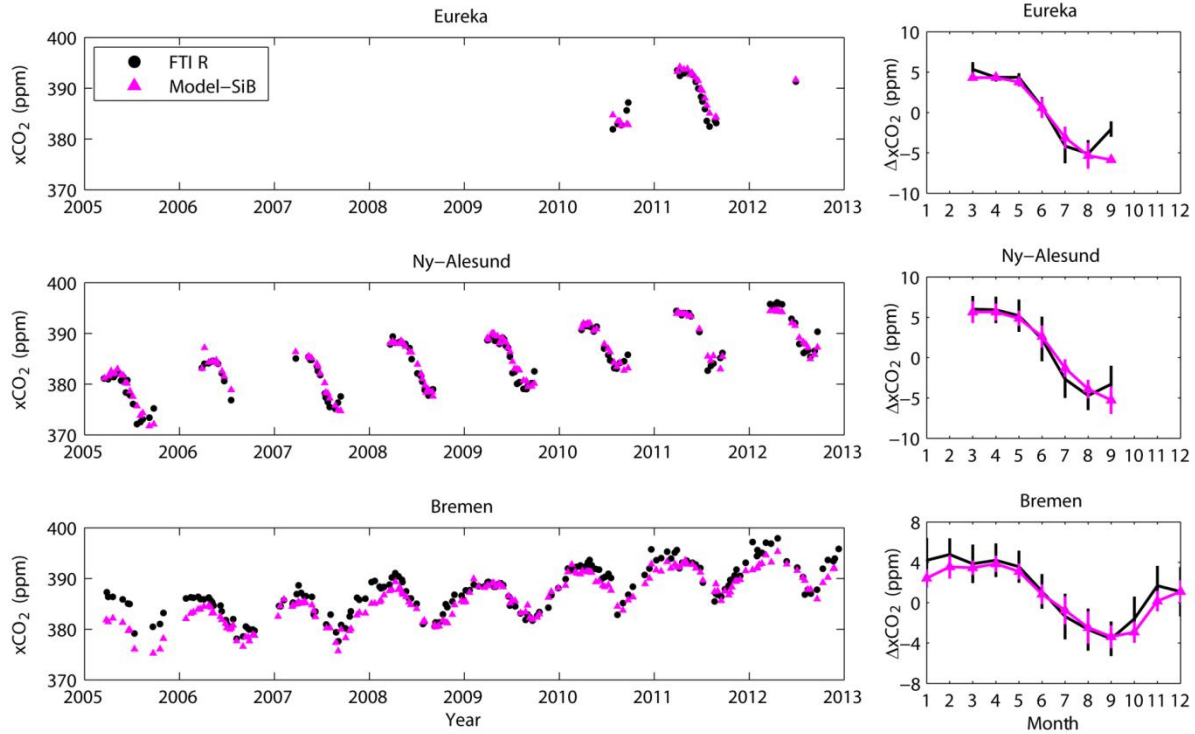
7

8

9

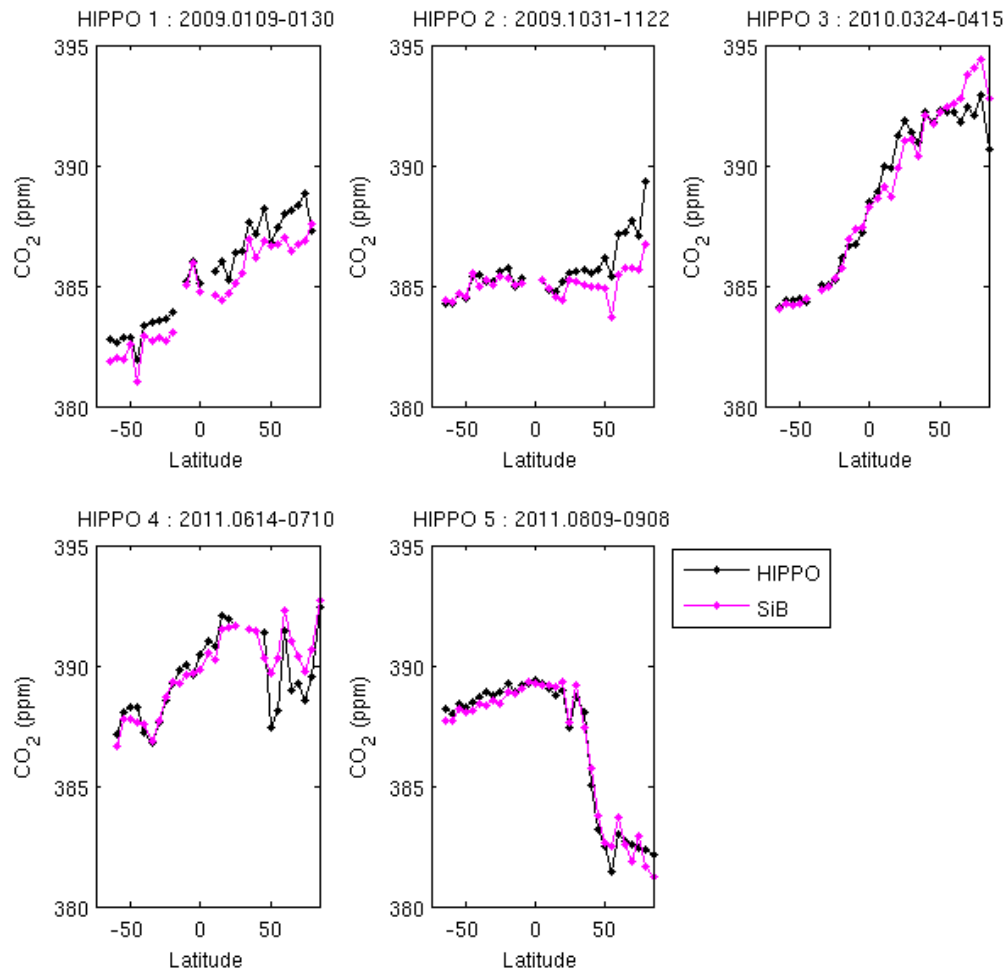
10

11



1  
 2 Figure 6. Comparison of FTIR measurements of CO<sub>2</sub> (black dots) to model simulations with SiB  
 3 land fluxes (magenta triangles) at Eureka, Ny-Ålesund and Bremen. The left panels show weekly  
 4 means from 2005 to 2012. The right panels show the monthly mean relative xCO<sub>2</sub> (relative to  
 5 annual mean) averaged for multiple years. The error bars are the standard deviations of each  
 6 month.

7  
 8  
 9  
 10  
 11  
 12  
 13  
 14  
 15



1  
 2 Figure 7. Comparison of HIPPO CO<sub>2</sub> measurements (black) and model simulations with SiB land  
 3 fluxes (magenta).